

# Single-Loop Deep Actor-Critic for Constrained Reinforcement Learning with Provable Convergence

Kexuan Wang, An Liu, *Senior Member, IEEE* and Baishuo Lin

**Abstract**—Deep actor-critic (DAC) algorithms, which combine actor-critic with deep neural network (DNN), have been among the most prevalent reinforcement learning algorithms for decision-making problems in simulated environments. However, the existing DAC algorithms are still not mature to solve realistic problems with non-convex stochastic constraints and high cost to interact with the environment. In this paper, we propose a single-loop DAC (SLDAC) algorithmic framework for general constrained reinforcement learning problems. In the actor module, the constrained stochastic successive convex approximation (CSSCA) method is applied to better handle the non-convex stochastic objective and constraints. In the critic module, the critic DNNs are only updated once or a few finite times for each iteration, which simplifies the algorithm to a single-loop framework. Moreover, the variance of the policy gradient estimation is reduced by reusing observations from the old policy. The single-loop design and the observation reuse effectively reduce the agent-environment interaction cost and computational complexity. Despite the biased policy gradient estimation incurred by the single-loop design and observation reuse, we prove that the SLDAC with a feasible initial point can converge to a Karush-Kuhn-Tucker (KKT) point of the original problem almost surely. Simulations show that the SLDAC algorithm can achieve superior performance with much lower interaction cost.

**Index Terms**—Constrained/Safe reinforcement learning, deep actor-critic, theoretical convergence.

## I. INTRODUCTION

### A. Background

The frameworks of reinforcement learning (RL) algorithms are typically categorized into three types: actor-only, critic-only, and actor-critic (AC). Among them, the AC is considered to have the most potential because it combines the strengths of the other two. Specifically, it alternates between the critic module which estimates the state-action value (Q value), and the actor module, which optimizes the policy using gradients calculated from the Q values provided by the critic module. Moreover, to handle the dimensional challenge in the case of large state and action spaces, modern AC algorithms often parameterize both the policy and the state-action value function (Q function) with deep neural networks (DNNs) [1], namely, deep actor-critic (DAC), which is the primary focus of this paper.

The DAC-based algorithms have achieved remarkable success in many sequential decision-making problems, such as playing Go [2] and Atari Games [3]. In these simulated environments, the agent learns to act by trial and error freely, as long as it brings performance improvement. However, in

many realistic domains such as Question-answering systems for medical emergencies [4], robot navigation [5], and radio resource management (RRM) in future 6G wireless communications [6], there are complicated stochastic constraints and high interaction cost with the environment. For example, the RRM in wireless communications needs to satisfy various quality of services (QoS) requirements such as average throughput and delay, which usually involve non-convex stochastic constraints. Moreover, each interaction with the wireless environment involves channel estimation and/or data transmission over wireless channels, which is quite resource-consuming. Naturally, the huge commercial interest in deploying the RL agent to realistic domains motivates the study of constrained reinforcement learning (CRL) with as few agent-environment interactions as possible.

A standard and well-studied formulation for the CRL problem mentioned above is the constrained Markov Decision Process (CMDP) [7]. In a CMDP, the agent attempts to maximize its expected total reward while ensuring constraints on expectations of auxiliary costs. A large body of works have been proposed for CMDPs [8]–[17], however, among which the DAC-based algorithms are still absent and far from mature. The classic DAC algorithms [17]–[20] for MDPs/CMDPs are generally developed under the two-loop framework, which constantly performs the critic update to accurately estimate the Q value for each iteration to avoid the accumulation of errors. However, the two-loop framework, as well as the commonly adopted on-policy sampling setting make the interaction between the agent and environment extremely costly. Furthermore, they usually simply adopt the stochastic (natural) gradient descent method to update policy without considering the non-convexity. In terms of theoretical analyses, to the best of our knowledge, no DAC-based algorithms for CMDPs have established a strictly global convergence guarantee. In fact, for the case of continuous action state space with policy parameterization, even other RL algorithms that are not based on the DAC framework can rarely guarantee the final convergence to the feasible set, except for our previous work [7].

To combat these weaknesses above, we propose a single-loop deep actor-critic (SLDAC) algorithm for CRL problems in this paper, where both the policy and the Q functions are parameterized by DNNs. In the actor module, considering the stochasticity and the non-convexity of the objective function and the constraints, the constrained stochastic successive convex approximation (CSSCA) method is adopted to replace the commonly used stochastic (natural) gradient descent in the existing DAC algorithms. In the critic module, we use the Temporal-Difference (TD) learning method to update the critic DNNs. To reduce the agent-environment interaction cost and computational complexity, we perform the critic update only

Kexuan Wang, An Liu, and Baishuo Lin are with the College of Information Science and Electronic Engineering, Zhejiang University, Hangzhou 310027, China (email: {kexuanWang, anliu, linbaishuo}@zju.edu.cn). (*Corresponding Author: An Liu*)

once or a few finite times for each iteration, which simplifies the algorithm to a single-loop framework (which is the so-called two-timescale framework). In particular, we also allow the observations generated by the old policy to be reused. Moreover, we manage to prove that the proposed SLDAC can converge to a Karush-Kuhn-Tucker (KKT) point of the original problem almost surely with a feasible initial point, even with a one-step critic update in each iteration.

### B. Related Works

In this section, we first review existing RL algorithms for CMDPs. Then, since there are few works on the theoretical analysis of DAC for CMDPs, we investigate the related works of DAC under unconstrained cases.

*RL Algorithms for CMDPs:* The major research lines of RL algorithms for CMDPs can be categorized into linear programming (LP) algorithms, primal-dual algorithms, and constrained policy optimization (CPO) algorithms based on the approach to policy optimization [21]. By utilizing the convexity of objective respect to state-action occupancy measure, works such as [9] and [8] propose a class of convergence-guaranteed algorithms based on LP method for CMDPs. However, the complexity and convergence rate of the LP-based algorithms are related to the size of the state and action space, and they are thus not applicable to more general problems with large state and action spaces. A common alternative of LP is the primal-dual method, which casts the CMDPs into an unconstrained max-min saddle-point problem and searches for the optimal policy in the primal-dual domain. However, the common shortcoming of this category of algorithms is that they cannot strictly guarantee the final convergence to the feasible set. Although [22] proves that the CRL problem for policies belonging to a general distribution class can be solved exactly in the convex dual domain, however, how to obtain the solution of non-convex optimization in the primal domain is not analyzed. [10]–[12] only establish value-average or policy-mixture convergence, which allows the agent to violate the safety constraints by oscillating around an optimal safety policy. To mitigate the oscillations, [13] and [14] propose a proportionally controlled Lagrangian method and an optimistic primal-dual proximal policy optimization algorithm, respectively. However, these two works have no theoretical convergence guarantees. The oscillation problem is partially solved by [15] but the constraint violations still exist. Although [16] provides a theoretical result of last-iterate convergence, it shows that the algorithm can only obtain a near-optimal final policy in the case of finite action states space with policy parameterization. In contrast, [7] proposes a novel successive convex approximation-based off-policy optimization (SCAOPO) algorithm, which addresses the CMDP problem by solving a sequence of convex objective/feasibility optimization problems and establishes a convergence guarantee to a KKT point, which greatly inspires this paper. However, the above works are not based on the DAC framework. Recently, authors in [17] connect the primal-dual method to two-loop DAC and propose the trust region policy optimization Lagrangian (TRPO-Lag) and proximal policy optimization Lagrangian (PPO-Lag), however, the global convergence of which is unknown. In addition, authors in [23] propose a CPO algorithm, which updates the policy within a trust region, but it also cannot theoretically assure a strictly feasible result.

Moreover, reinforcement learning algorithms for CMDPs can also be divided into online CRL [24] and offline CRL [25] from the perspective of data acquisition, where the former aims to learn a task-solving policy by interacting with the environment, while the later chooses to learn from offline datasets. Due to the discrepancy between the offline dataset and the real-world environment, the offline CRL is usually only suited for the pre-training stage. Therefore, we mainly focus on the online setting in this paper, while leaving the research of the offline setting in our future work.

*Convergence Analysis for Deep Actor-Critic:* A large body of works establishes the convergence guarantee for DAC in the unconstrained case, i.e., [18]–[20] for two-loop DAC and [26]–[28] for the so-called single-loop (two-timescale) DAC. Recently, authors in [29] propose the single-timescale DAC, which further proves that the actor module and the critic module can converge on the same timescale. However, all the above DAC algorithms simply adopt the stochastic (natural) policy descent, which makes them only suitable for simple constraints with deterministic convex feasible sets. In addition, the challenging observation reuse setting is rarely considered.

### C. Contributions

The contributions in this paper are summarized below:

- **Non-convex Constrained Optimization and Low-cost Settings:** Compared with the existing DAC algorithms, the proposed SLDAC pays more attention to addressing the requirements of CRL problems in the realistic domains. There are two major differences/advantages: 1) our method takes into account the stochasticity and the non-convexity of both the objective function and the constraints; 2) the combination of single-loop framework and the observation reuse can significantly reduce the agent-environment interaction cost and computational complexity.
- **Theoretical Convergence Analysis of SLDAC:** Under some technical conditions, we prove that the proposed SLDAC can converge to KKT points of the original CMDP problem with a feasible initial point, despite the biased estimation induced by the observation reuse and the single-loop framework. To the best of our knowledge, it is the first single-loop DAC algorithm for CMDPs that can provably converge to a KKT point. Moreover, we also provide some valuable theoretical results, including the asymptotic consistency of the estimated function values and policy gradients, as well as the finite-time convergence rates of both the critic DNNs.

The rest of the paper is organized as follows. Section II briefly introduces some preliminaries, including general formulations of CRL, neural network parameterization, and assumptions on problem structure. The SLDAC algorithmic framework and its convergence analysis are presented in Sections III and IV, respectively. Section V provides simulation results and the conclusion is drawn in section VII.

## II. PRELIMINARIES

In this section, we first introduce some preliminaries of CMDP and then briefly introduce a family of DNNs, which are commonly used in modern algorithms to parameterize

the policy  $\pi$  and Q functions. Moreover, we make several assumptions on the problem structure, before we present the algorithmic framework.

### A. Problem Formulation

A CMDP can be denoted as a tuple  $(\mathcal{S}, \mathcal{A}, P, C)$ , where  $\mathcal{S} \subseteq \mathbb{R}^{n_s}$  is the state space,  $\mathcal{A} \subseteq \mathbb{R}^{n_a}$  is the action space,  $P : \mathcal{S} \times \mathcal{A} \times \mathcal{S} \rightarrow [0, 1]$  is the transition probability function, where  $P(s' | s, a)$  denotes the probability of transition to state  $s'$  from state  $s \in \mathcal{S}$  with an action  $a \in \mathcal{A}$ , and  $C_{i=0,1,\dots} : \mathcal{S} \times \mathcal{A} \rightarrow \mathbb{R}$  are the per-stage reward/cost functions. The policy  $\pi : \mathcal{S} \rightarrow \mathbf{P}(\mathcal{A})$  is a map from states to an action probability distribution, with  $\pi(a | s)$  denoting the probability of selecting action  $a \in \mathcal{A}$  in state  $s \in \mathcal{S}$ . Then, the transition probability  $P$  and policy  $\pi$  together determine the probability distribution of the trajectory  $\{s_0, a_0, s_1, \dots\}$ , where  $s_t$  and  $a_t$  denote the state and action at time step  $t$ . For simplicity, we denote the probability distribution over the trajectory by  $p_\pi$ , i.e.,  $s_t \sim P(\cdot | s_{t-1}, a_{t-1})$ ,  $a_t \sim \pi(\cdot | s_t)$ .

Because of the curse of dimension, we parameterize the policy  $\pi$  with DNN over  $\theta \in \Theta$ , and then we denote the parameterized policy as  $\pi_\theta$ . With the  $\pi_\theta$ , the goal of a general CRL problem for continuous control can be formulated based on the CMDP as:

$$\begin{aligned} \min_{\theta \in \Theta} J_0(\theta) &\triangleq \lim_{T \rightarrow \infty} \frac{1}{T} \mathbb{E}_{p_{\pi_\theta}} \left[ \sum_{t=0}^{T-1} C_0(s_t, a_t) \right] \\ \text{s.t. } J_i(\theta) &\triangleq \lim_{T \rightarrow \infty} \frac{1}{T} \mathbb{E}_{p_{\pi_\theta}} \left[ \sum_{t=0}^{T-1} C_i(s_t, a_t) \right] - c_i \leq 0. \end{aligned} \quad (1)$$

where  $c_1, \dots, c_I$  denote the constraint values. Problem (1) embraces many important applications, which are specifically exemplified in the following.

*Example 1 (Delay-Constrained Power Control for Downlink MU-MIMO system):* Some mission-critical applications in the forthcoming 6G communication, such as Internet-of-Things and virtual reality applications, are emerging and call for low-delay communication services for each user [30]–[32]. Now we consider a delay-constrained power control problem, which aims to obtain a policy  $\pi_\theta$  to satisfy this stringent requirement with minimal long-term average power consumption. Consider a downlink MU-MIMO system consisting of a  $N_t$ -antennas base station (BS) and  $K$  single-antenna users ( $N_t \geq K$ ), where the BS maintains  $K$  dynamic data queues for the burst traffic flows to each user. Suppose that the time dimension is partitioned into decision slots indexed by  $t$  with slot duration  $t_0$ , and each queue dynamic of the  $k$ -user has a random arrival data rate  $A_k(t)$ , where  $E[A_k] = \lambda_k$ . The data rate  $R_k(t)$  of user  $k$  is given by

$$R_k = B \log_2 \left( 1 + \frac{P_k |\mathbf{h}_k^H \mathbf{v}_k(\alpha_Z)|^2}{\sum_{j \neq k} P_j |\mathbf{h}_k^H \mathbf{v}_j(\alpha_Z)|^2 + \sigma_k^2} \right),$$

where we omit the time slot index for conciseness,  $B$  denotes the bandwidth,  $\mathbf{h}_k$  is the downlink channel of the  $k$ -th user,  $\sigma_k^2$  is the noise power at the  $k$ -th user,  $P_k$  is the power allocated to the  $k$ -th user, and  $\mathbf{v}_k(\alpha_Z)$  is the normalized regularized zero-forcing (RZF) precoder with regularization factor  $\alpha_Z$  [33]. Then, the queue dynamic of the  $k$ -user  $Q_k(t)$  is given by

$$Q_k(t) = \max \left\{ A_k(t) t_0 - R_k(t) t_0 + Q_k(t-1), 0 \right\}.$$



Figure 1. An autonomous vehicle transport environment provided by the Safety Gym.

Finally, the delay-constrained power control problem can be formulated as

$$\begin{aligned} \min_{\theta \in \Theta} J_0(\theta) &\triangleq \lim_{T \rightarrow \infty} \frac{1}{T} \mathbb{E}_{p_{\pi_\theta}} \left[ \sum_{t=1}^T \sum_{k=1}^K P_k(t) \right] \\ \text{s.t. } J_i(\theta) &\triangleq \lim_{T \rightarrow \infty} \frac{1}{T} \mathbb{E}_{p_{\pi_\theta}} \left[ \sum_{t=1}^T \frac{Q_k(t)}{\lambda_k} \right] - c_k \leq 0, \forall k, \end{aligned} \quad (2)$$

where  $c_1, \dots, c_K$  denote the maximum allowable average delay for each user. In this case, the BS at the  $t$ -th time slot obtains state information  $\mathbf{s}_t = \{\mathbf{Q}(t), \mathbf{H}(t)\}$ , where  $\mathbf{Q} = [Q_1, \dots, Q_K]^T \in \mathbb{R}^K$  and  $\mathbf{H} = [\mathbf{h}_1, \dots, \mathbf{h}_K]^H \in \mathbb{C}^{K \times N_t}$ , and takes action  $\mathbf{a}_t = \{\mathbf{P}_t(t), \alpha_Z(t)\}$  according to policy  $\pi_\theta$ , where  $\mathbf{P}_t = [P_1, \dots, P_K]$ . Moreover, the reward function  $C_0(s_t, \mathbf{a}_t) = \sum_{k=1}^K P_k(t)$ , and the cost function  $C_1(s_t, \mathbf{a}_t) = \frac{Q_k(t)}{\lambda_k}$ .

*Example 2 (Autonomous Vehicle Transport with Safety Assurance):* Autonomous vehicles with safety assurance have attracted significant attention in recent years. To prepare for its application in the real world, the OpenAI Safety Gym [17] provides a widely used benchmarking simulated environment, as shown in Fig. 3b. A car robot with two independently driven parallel wheels and a free-rolling rear wheel is required to find the yellow box and transport it to the green destination while avoiding hazards (including 4 blue areas representing primary hazards and 4 blue pillars representing) as much as possible. In this case, the current state  $s_t$  is obtained by onboard radar and includes the distance and direction information of surrounding objects and hazardous areas. The action  $\mathbf{a}_t$  is adopted to control the two independently driven parallel wheels of the car. The reward  $C_0(s_t, \mathbf{a}_t)$  obtained by the robot consists of a small, dense component encouraging movement toward the box and the target goal and a large, sparse component for successfully completing the task. Conversely, each time the car enters a blue zone, it receives a cost of  $C_1(s_t, \mathbf{a}_t)=1$ , and each time it touches a blue pillar, it receives a cost of  $C_1(s_t, \mathbf{a}_t)=10$ . Moreover, the constraint for this problem is that the average cost is less than or equal to  $c_1$ .

*Example 3 (Constrained Linear-Quadratic Regulator):* The constrained Linear-quadratic regulator (CLQR) is one of the most fundamental problems in control theory [34]. According to [35] and [7], by denoting  $\mathbf{s}_t \in \mathbb{R}^{n_s}$  and  $\mathbf{a}_t \in \mathbb{R}^{n_a}$  as the state and action of CLQR problem at the time  $t$ , the objective cost and the constraint cost in the CLQR

setting are respectively given by

$$C_0(\mathbf{s}_t, \mathbf{a}_t) = \mathbf{s}_t^\top Q_0 \mathbf{s}_t + \mathbf{a}_t^\top R_0 \mathbf{a}_t,$$

$$C_1(\mathbf{s}_t, \mathbf{a}_t) = \mathbf{s}_t^\top Q_1 \mathbf{s}_t + \mathbf{a}_t^\top R_1 \mathbf{a}_t,$$

where  $\{Q_0, R_0, Q_1, R_1\}$  are semi-positive definite matrices, the state  $\mathbf{s}_{t+1} = \mathbf{X}\mathbf{s}_t + \mathbf{Y}\mathbf{a}_t + \epsilon_t$  with transition matrices  $\mathbf{X} \in \mathbb{R}^{n_s \times n_s}$  and  $\mathbf{Y} \in \mathbb{R}^{n_s \times n_a}$ , and  $\{\epsilon_t\}$  is the process noise.

*Remark 1. (Infinite-horizon average reward/cost criterion:)* There are two reward/cost criteria are studied in RL algorithms, i.e., the infinite-horizon average reward/cost criterion and the  $\gamma$ -discounted reward/cost criterion. We adopt the former mainly because it is more challenging in theoretical analysis. Convergence analysis techniques for the discounted reward setting, such as backward induction and  $\gamma$ -contraction, cannot be applied to the infinite-horizon average reward/cost setting [36]. In contrast, the extension from the former to the latter is generally considered trivial [26], both in algorithmic design and theoretical analysis.

### B. Neural Network Parameterization

Following the same standard setup implemented in line with recent works [37]–[39], we consider such an  $L$ -hidden-layer neural network:

$$f_m(\boldsymbol{\alpha}; \mathbf{x}) = \sqrt{m} \mathbf{W}_L \sigma(\mathbf{W}_{L-1} \cdots \sigma(\mathbf{W}_1 \phi(\mathbf{x})) \cdots), \quad (3)$$

where the subscript  $m$  is the width of the neural network,  $\sigma(\cdot)$  is the entry-wise activation function,  $\phi(\cdot)$  is a feature mapping of the input data  $\mathbf{x} \in \mathbb{R}^d$ , and the input data is usually normalized, i.e.,  $\|\mathbf{x}\|_2 \leq 1$ . Moreover,  $\mathbf{W}_1 \in \mathbb{R}^{m \times d_{in}}$ ,  $\mathbf{W}_L \in \mathbb{R}^{d_{out} \times m}$  and  $\mathbf{W}_l \in \mathbb{R}^{m \times m}$  for  $l = 2, \dots, L-1$  are parameter matrices, and  $\boldsymbol{\alpha} = (\text{vec}(\mathbf{W}_1)^\top, \dots, \text{vec}(\mathbf{W}_L)^\top)$  is the concatenation of the vectorization of all the parameter matrices. It is easy to verify that  $\|\boldsymbol{\alpha} - \boldsymbol{\alpha}'\|_2^2 = \sum_{l=1}^L \|\mathbf{W}_l - \mathbf{W}_l'\|_F^2$ . For simplicity, we assume that different layers in a network have the same width  $m$ . Remark that our results can be easily generalized to many other activation functions and the setting that the widths of each layer are not equal.

In this paper, we parameterize both the policy and Q-functions with the DNNs defined above. Specifically, in the actor module, we employ the commonly used Gaussian policy [40, Chapter 13.7] with mean  $\boldsymbol{\mu}$  and diagonal elements of the covariance matrix  $\boldsymbol{\Sigma}$  parameterized by  $f_{m_\mu}(\boldsymbol{\theta}_\mu; \mathbf{s}) = \mathbb{R}^{n_a}$  and  $f_{m_\sigma}(\boldsymbol{\theta}_\sigma; \mathbf{s}) \subseteq \mathbb{R}^{n_a}$ , respectively, and keep the non-diagonal elements of  $\boldsymbol{\Sigma}$  as 0. That is,

$$\pi_\theta(\mathbf{a} | \mathbf{s}) \propto |\boldsymbol{\Sigma}|^{-\frac{1}{2}} \exp\left(-\frac{1}{2}(\boldsymbol{\mu} - \mathbf{a})^\top \boldsymbol{\Sigma}^{-1}(\boldsymbol{\mu} - \mathbf{a})\right), \quad (4)$$

where the policy parameter  $\boldsymbol{\theta} = [\boldsymbol{\theta}_\mu, \boldsymbol{\theta}_\sigma] \in \Theta$ . In the critic module, we adopt dual critic DNNs  $f_{m_Q}(\boldsymbol{\omega}^i; \mathbf{s}, \mathbf{a}) \subseteq \mathbb{R}$  and  $f_{m_Q}(\bar{\boldsymbol{\omega}}^i; \mathbf{s}, \mathbf{a}) \subseteq \mathbb{R}$  to approximate the  $i$ -th Q function. Please note that different Q functions are parameterized by the same DNNs, but with different parameters. For simplification, we abbreviate  $f_{m_Q}(\boldsymbol{\omega}; \mathbf{s}, \mathbf{a})$  to  $f(\boldsymbol{\omega})$  throughout this paper when no confusion arises.

### C. Important Assumptions on the Problem Structure

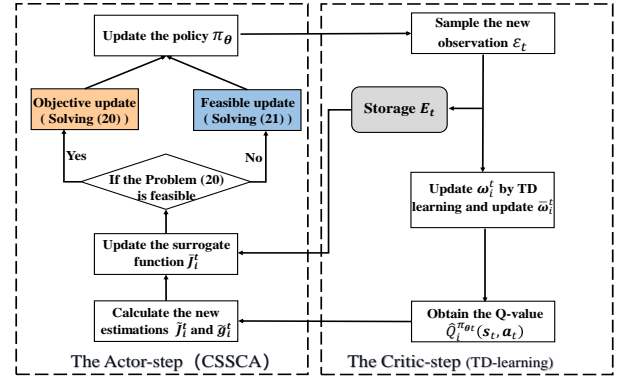


Figure 2. The algorithmic framework of the proposed SLDAC

*Assumption 1. (Assumptions on the Problem Structure)(Assumptions on the Problem Structure:)*

1) There are constants  $\lambda > 0$  and  $\rho \in (0, 1)$  satisfying

$$\sup_{\mathbf{s} \in \mathcal{S}} d_{TV}(\mathbf{P}(\mathbf{s}_t | \mathbf{s}_0 = \mathbf{s}), \mathbf{P}_{\pi_\theta}) \leq \lambda \rho^t, \quad (5)$$

for all  $t = 0, 1, \dots$ , where  $\mathbf{P}_{\pi_\theta}$  is the stationary state distribution under policy  $\pi_\theta$  and  $d_{TV}(\mu, \nu) = \int_{\mathcal{S} \in \mathcal{S}} |\mu(d\mathbf{s}) - \nu(d\mathbf{s})|$  denotes the total-variation distance between the probability measures  $\mu$  and  $\nu$ .

2) State space  $\mathcal{S} \subseteq \mathbb{R}^{n_s}$  and action space  $\mathcal{A} \subseteq \mathbb{R}^{n_a}$  are both compact. The costs/rewards  $C_i, \forall i$ , are bounded.

3) The gradients of  $J_i(\boldsymbol{\theta}), \forall i$ , are uniformly bounded and follow Lipschitz continuity over the parameter  $\boldsymbol{\theta} \in \Theta$ .

4) The DNNs' parameter spaces  $\Theta \subseteq \mathbb{R}^{n_\theta}$  and  $\Omega_i \subseteq \mathbb{R}^{n_\omega}, \forall i$  are compact and convex, and the outputs of DNNs are bounded.

5) The policy  $\pi_\theta$  follows Lipschitz continuity over the parameter  $\boldsymbol{\theta} \in \Theta$ .

Assumption 1-1) controls the bias caused by the Markovian noise in the observations by assuming the uniform ergodicity of the Markov chain generated by  $\pi_\theta$ , which is a standard requirement in the literature, see e.g., [41], [42] and [7]. Assumption 1-2) considers a general scenario in which the state and action spaces can be continuous. Assumption 1-3) holds based on the condition that the gradient of DNNs with respect to parameters are bounded and satisfy Lipschitz continuity. Remark this condition can be satisfied by a large category of DNNs with Lipschitz-smooth activation functions and over-parameterized DNNs using the rectified linear unit (ReLU) function [38]. Assumption 1-4) is trivial in CRL problems. Assumption 1-5) can be easily satisfied as long as there is no gradient explosion during the training process. Some techniques such as proper initialization and gradient clipping can help avoid gradient explosion [43]–[45].

### III. SLDAC ALGORITHMIC FRAMEWORK

As illustrated in Fig. 2, the proposed SLDAC algorithm performs iterations between the critic module and the actor module. At the  $t$ -th iteration, the new observation  $\epsilon_t$  is used to update the critic module, and old observations in  $E_t$  are allowed to be reused to update the actor module. In the following, we elaborate on the sampling and storage, as well as the design of the actor and critic modules in detail. The overall SLDAC algorithm is summarized in Algorithm 1 and

for readers' convenience, the meanings of some important symbols hereafter are listed in Table I.

### A. Sampling and Storage

Once given the current policy  $\pi_{\theta_t}$ , the agent at state  $s_t$  can choose an action  $\mathbf{a}_t$  according to the policy  $\pi_{\theta_t}$  and transitions to the next new state  $s_{t+1}$  with the environment feeding back a set of cost (reward) function values  $\{C_i(s_t, \mathbf{a}_t)\}_{i=0, \dots, I}$ . Then, we denote the tuple  $\varepsilon_t = \{s_t, \mathbf{a}_t, \{C_i(s_t, \mathbf{a}_t)\}_{i=0, \dots, I}, s_{t+1}\}$  as a new observation at the  $t$ -th iteration and store the latest  $T_t$  observations in the storage  $E_t$ , i.e.,  $E_t = \{\varepsilon_{t-T_t+1}, \varepsilon_{t-T_t+2}, \dots, \varepsilon_t\}$ . In practice, a minibatch of  $B$  new observations can be obtained by performing this interaction repeatedly under  $\pi_{\theta_t}$ , to perform a few finite  $q < B$  critic updates at each iteration, where  $B/q$  new observations are used in each critic update. The batch size  $B$  and the number of inner iterations  $q$  can be properly chosen to achieve a flexible tradeoff between better estimation accuracy for the Q values/policy gradient and the interaction cost with the environment as well as the computational complexity. In the algorithm design and convergence analyses of this paper, we only focus on the most challenging case when  $B = q = 1$  for clarity. However, the scheme and theoretical result also hold for arbitrary choice of  $B \geq q \geq 1$ .

### B. The Critic Module

We first denote  $C_0(s_t, \mathbf{a}_t) = C_0(s_t, \mathbf{a}_t)$  and  $C_i'(s_t, \mathbf{a}_t) = C_i(s_t, \mathbf{a}_t) - c_i, i = 1, \dots, I$ . For any  $\pi_{\theta_t}$ , there is a set of Q functions  $\{Q_i^{\pi_{\theta_t}}\}_{i=0, \dots, I}$  defined as

$$Q_i^{\pi_{\theta_t}}(s, \mathbf{a}) = \mathbb{E}_{p_t} \left[ \sum_{l=0}^{\infty} \left( C_i'(s_l, \mathbf{a}_l) - J_i(\theta_t) \right) \middle| s_0 = s, \mathbf{a}_0 = \mathbf{a} \right], \forall i, s, \mathbf{a}, \quad (6)$$

where we denote the distribution  $p_{\pi_{\theta_t}}$  by  $p_t$  for short. Since it is unrealistic to obtain  $J_i(\theta_t)$  online, we redefine a set of surrogate Q functions  $\{\hat{Q}_i^{\pi_{\theta_t}}\}_{i=0, \dots, I}$  as

$$\hat{Q}_i^{\pi_{\theta_t}}(s, \mathbf{a}) = \mathbb{E}_{p_t} \left[ \sum_{l=0}^{\infty} \left( C_i'(s_l, \mathbf{a}_l) - \hat{J}_i^t \right) \middle| s_0 = s, \mathbf{a}_0 = \mathbf{a} \right], \forall i, s, \mathbf{a}, \quad (7)$$

where  $\hat{J}_i^t$  is the estimate of  $J_i(\theta_t)$  that will be given in (15) and be proved that  $\lim_{t \rightarrow \infty} |\hat{J}_i^t - J_i(\theta_t)| = 0$ . To approximate  $\{\hat{Q}_i^{\pi_{\theta_t}}\}_{i=0, \dots, I}$ , we adopt two sets of critic DNNs and update them as follows.

The first set of DNNs  $\{f(\omega^i)\}_{i=0, \dots, I}$  is updated to minimize the mean-squared projected Bellman error (MSBE) [41]:

$$\min_{\omega_t^i} \mathbb{E}_{\sigma_{\pi_{\theta_t}}} \left[ \left( f(\omega_t^i; s_t, \mathbf{a}_t) - \mathcal{T}_t f(\omega_t^i; s_t, \mathbf{a}_t) \right)^2 \right], \forall i, \quad (8)$$

where  $\sigma_{\pi_{\theta_t}}(s_t, \mathbf{a}_t) = \pi_{\theta_t}(\mathbf{a}_t | s_t) \cdot \mathbf{P}_{\pi}(s_t)$  is the stationary state-action distribution, and we abbreviate it as  $\sigma_t$ . In addition, the Bellman operator  $\mathcal{T}_t$  is defined as

$$\mathcal{T}_t f(\omega_t^i; s_t, \mathbf{a}_t) = \mathbb{E}_{p_t} \left[ f(\omega_t^i; s_{t+1}, \mathbf{a}'_{t+1}) + C_i'(s_t, \mathbf{a}_t) - \hat{J}_i^t, \forall i, \right] \quad (9)$$

where  $\mathbf{a}'_{t+1}$  is the action chosen by current policy  $\pi_{\theta_t}$  at the next state  $s_{t+1}$ . To solve Problem (8), we first define a neighborhood of the randomly initialized parameter  $\omega_0^i, \forall i$  as

$$\mathbb{B}(\omega_0^i, R_\omega) = \left\{ \omega^i = \left( \text{vec}(\mathbf{W}_1^i)^\top, \dots, \text{vec}(\mathbf{W}_L^i)^\top \right)^\top : \left\| \mathbf{W}_l^i - \mathbf{W}_l^{i,(0)} \right\|_F \leq R_\omega, l = 1, \dots, L \right\}, \quad (10)$$

where  $\mathbf{W}_l^{i,(0)}$  is the parameter of the  $l$ -th layer corresponding to  $\omega_0^i$ . Then, we update the parameter  $\omega^i$  in the neighborhood  $\mathbb{B}(\omega_0^i, R_\omega)$  using the TD-learning method:

$$\omega_t^i = \Pi_{\Omega_i}(\omega_{t-1}^i - \eta_t \Delta_i^{\omega_{t-1}^i}), \forall i, \quad (11)$$

where  $\{\eta_t\}$  is a decreasing sequence satisfying Assumption 2 in section IV-A,  $\Pi_{\Omega_i}$  is a projection operator that projects the parameter into the constraint set  $\Omega_i \triangleq \mathbb{B}(\omega_0^i, R_\omega)$ , and the stochastic gradient  $\Delta_i^{\omega_{t-1}^i}, \forall i$  is defined as

$$\Delta_i^{\omega_{t-1}^i} = \left( f(\omega_{t-1}^i; s_t, \mathbf{a}_t) - (C_i'(s_t, \mathbf{a}_t) - \hat{J}_i^{t-1} + f(\omega_{t-1}^i; s_{t+1}, \mathbf{a}'_{t+1})) \right) \nabla_{\omega} f(\omega_{t-1}^i; s_t, \mathbf{a}_t). \quad (12)$$

To enhance stability, we adopt the other set of critic networks  $\{f(\bar{\omega}^i)\}_{i=0, \dots, I}$  and use their outputs to calculate the policy gradients in the actor module. The parameter  $\bar{\omega}^i$  is updated by the following recursive operation from the 0-th iteration  $\bar{\omega}_0^i = \omega_1^i$ :

$$\bar{\omega}_t^i = (1 - \gamma_t) \bar{\omega}_{t-1}^i + \gamma_t \omega_t^i, \forall i, \quad (13)$$

where  $\{\gamma_t\}$  is also decreasing sequence satisfying the Assumption 2 in section IV-A.

Table I  
MEANINGS OF IMPORTANT SYMBOLS

Symbol	Meaning
$\hat{J}_i^t / \hat{g}_i^t$	New estimate of the function value/gradient to update $\hat{J}_i^t / \hat{g}_i^t$
$\tilde{J}_i^t / \tilde{g}_i^t$	Estimate of the function value/gradient to construct $\tilde{J}_i^t$
$J_i(\theta_t), \tilde{J}_i^t$	Original objective function and its surrogate function
$Q_i^{\pi_{\theta_t}}, \hat{Q}_i^{\pi_{\theta_t}}$	Exact Q-function and its surrogate function calculated by $\hat{J}_i^t$
$\omega_t, \bar{\omega}_t$	Parameters for the dual sets of critic networks
$f(\omega_t^i), f(\bar{\omega}_t^i)$	Dual sets of critic networks to approximate $\hat{Q}_i^{\pi_{\theta_t}}$
$\mathbf{m}, \bar{\mathbf{m}}$	Auxiliary parameters for $\omega_t$ and $\bar{\omega}_t$
$\hat{f}(\bar{\omega}_t^i)$	Local linearization function of $f(\bar{\omega}_t^i)$
$\varepsilon_t, E_t$	New observation and its storage under $\pi_{\theta_t}$
$\bar{\varepsilon}_t, \bar{E}_t$	Auxiliary observation and its storage under fixed $\pi_{\theta_{t-n_t}}$

### C. The Actor Module

The key to solving (1) in the actor step is to replace the objective/constraint functions  $\{J_i(\theta), \forall i\}$  by some convex surrogate functions  $\{\tilde{J}_i^t(\theta), \forall i\}$  constructed by the estimated function values  $\{\hat{J}_i^t, \forall i\}$  and the estimated policy gradients  $\{\hat{g}_i^t, \forall i\}$ . Then, the original problem is addressed by solving a sequence of convex optimization problems.

The surrogate function  $\tilde{J}_i^t(\theta)$  can be seen as a convex approximation of  $J_i(\theta)$  based on the  $t$ -th iterate  $\theta_t$ , which is formulated as:

$$\tilde{J}_i^t(\theta) = \hat{J}_i^t + (\hat{g}_i^t)^\top (\theta - \theta_t) + \zeta_i \|\theta - \theta_t\|_2^2, \forall i, \quad (14)$$

where  $\zeta_i$  is a positive constant,  $\hat{J}_i^t \in \mathbb{R}$  is the estimate of  $J_i(\theta)$ , and  $\hat{g}_i^t \in \mathbb{R}^{n_{\theta_i}}$  is the estimate of gradient  $\nabla J_i(\theta)$  at the  $t$ -th iteration, which are updated by

$$\hat{J}_i^t = (1 - \alpha_t) \hat{J}_i^{t-1} + \alpha_t \tilde{J}_i^t, \forall i, \quad (15)$$

$$\hat{g}_i^t = (1 - \alpha_t) \hat{g}_i^{t-1} + \alpha_t \tilde{g}_i^t, \forall i, \quad (16)$$

where the step size  $\{\alpha_t\}$  is a decreasing sequence satisfying the Assumption 2 in Section IV,  $\tilde{J}_i^t$  and  $\tilde{g}_i^t$  are the realizations of function value and its gradient whose specific forms are given below.

To reduce the estimation variance and use the observations more efficiently, we propose an off-policy estimation strategy in which  $\tilde{J}_i^t$  and  $\tilde{g}_i^t$  can be obtained by reusing old observations in  $E_t$ . By the sample average method, we can first obtain the new estimation of function value at the  $t$ -th iteration  $\tilde{J}_i^t$ :

$$\tilde{J}_i^t = \frac{1}{T_t} \sum_{l=1}^{T_t} C_i'(s_{t-T_t+l}, \mathbf{a}_{t-T_t+l}), \forall i. \quad (17)$$

Then according to the policy gradient theorem [46], we have

$$\nabla J_i(\theta) = \mathbb{E}_{\sigma_{\pi_{\theta}}} [Q_i^{\pi_{\theta}}(s, \mathbf{a}) \nabla_{\theta} \log \pi_{\theta}(\mathbf{a} | s)], \forall i. \quad (18)$$

We adopt the idea of the sample average and give the estimate of the gradient at the  $t$ -th iteration as

$$\tilde{g}_i^t = \frac{1}{T_t} \sum_{l=1}^{T_t} f(\bar{\omega}_i^t; s_{t-T_t+l}, \mathbf{a}_{t-T_t+l}) \cdot \nabla_{\theta} \log \pi_{\theta}(\mathbf{a}_{t-T_t+l} | s_{t-T_t+l}), \forall i. \quad (19)$$

Based on the surrogate functions  $\{\tilde{J}_i^t(\theta)\}_{i=0, \dots, I}$ , the optimal solution  $\bar{\theta}_t$  of the following problem is solved:

$$\begin{aligned} \bar{\theta}_t &= \operatorname{argmin}_{\theta \in \Theta} \bar{J}_0^t(\theta) \\ \text{s.t. } &\bar{J}_i^t(\theta) \leq 0, i = 1, \dots, I. \end{aligned} \quad (20)$$

If problem (20) turns out to be infeasible, the optimal solution  $\bar{\theta}_t$  of the following convex problem is solved:

$$\begin{aligned} \bar{\theta}_t &= \operatorname{argmin}_{\theta \in \Theta, y} y \\ \text{s.t. } &\bar{J}_i^t(\theta) \leq y, i = 1, \dots, I. \end{aligned} \quad (21)$$

Please note that the surrogate problems (20) and (21) both belong to the convex quadratic problem with a closed-form solution, which can be easily solved by standard convex optimization algorithms, e.g. Lagrange-dual methods. Then, once given  $\bar{\theta}_t$ ,  $\theta_{t+1}$  is updated according to

$$\theta_{t+1} = (1 - \beta_t) \theta_t + \beta_t \bar{\theta}_t. \quad (22)$$

where the step size  $\{\beta_t\}$  is a decreasing sequence satisfying Assumption 2 in Section IV.

#### D. Key Differences from Closely Related Works

As we mentioned in section I-B, several advanced CRL algorithms have been designed, e.g. TRPO-Lag and PPO-Lag [17], CPO [23], and our previous work [7]. However, there are still key differences in algorithm design between this paper and these closely related works, as illustrated in Table II.

TRPO-Lag, PPO-Lag, and CPO are all advanced DAC algorithms for CMDPs. However, they do not have a special

---

#### Algorithm 1 Single-Loop Deep Actor-Critic Algorithm

---

**Input:** The decreasing sequences  $\{\alpha_t\}$ ,  $\{\beta_t\}$ ,  $\{\eta_t\}$ , and  $\{\gamma_t\}$ , randomly generate the initial entries of  $\omega_0^i$  and  $\theta_0$  from  $\mathcal{N}(0, 1/m^2)$ .

**for**  $t = 0, 1, \dots$  **do**

    Sample the new observation  $\varepsilon_t$  and update the storage  $E_t$ .

**Critic Step:**

        Update  $\omega_t^i$  and  $\bar{\omega}_t^i$  by (11) and (13), respectively.

**Actor Step:**

        Calculate  $\hat{J}_i^t$  according to (17) and (15).

        Estimate gradient  $\hat{g}_i^t$  according to (19) and (16).

        Update the surrogate function  $\{\tilde{J}_i^t(\theta)\}_{i=0, \dots, I}$  via (14).

**if** Problem (20) is feasible:

            Solve (20) to obtain  $\bar{\theta}_t$ .

**else**

            Solve (21) to obtain  $\bar{\theta}_t$ .

**end if**

        Update policy parameters  $\theta_{t+1}$  according to (22).

**end for**

---

Table II  
KEY DIFFERENCES FROM CLOSELY RELATED WORKS

Algorithm for CMDPs	Framework	Observation reuse	Convergence to a KKT point
DAC in [17], [23]	Two-loop AC	×	×
SCAOPO in [7]	Actor-only	✓	✓
SLDAC in this paper	Single-loop AC	✓	✓

design for step sizes as Assumption 2 in this paper and therefore belong to the two-loop AC, that is,  $B \rightarrow \infty$  and  $q \rightarrow \infty$  (or  $B$  and  $q$  are sufficiently large in practice) are required to avoid error accumulation, which leads to high interaction cost. Moreover, they adopt on-policy sampling and their approaches to policy optimization make them only suitable for simple convex constraints. Both the SCAOPO in [7] and the SLDAC in this paper allow the observation reuse to improve the observation efficiency, adopt the CSSCA to better handle the non-convexity of objective and constraints and guarantee the final convergence to a KKT point (up to an error of  $\epsilon_{m_Q}$  with  $\lim_{m_Q \rightarrow \infty} \epsilon_{m_Q} = 0$ ). However, the SCAOPO is based on the actor-only framework, which simply adopts the MC method to estimate Q values. Instead of the MC method, we use dual DNNs to approximate Q functions, which reduces variance and tends to find more accurate estimates. These innovative designs of SLDAC help to achieve superior performance with much lower interaction cost, although it makes convergence analysis more challenging.

#### IV. CONVERGENCE ANALYSIS

In the following, we first present the key assumptions on step sizes and then analyze the convergence rate of the critic module. Based on this theoretical result and assumptions above, we further show that the surrogate functions satisfy asymptotic consistency. Finally, we prove that the proposed Algorithm 1 converges to a KKT point (up to an error of  $\epsilon_{m_Q}$  with  $\lim_{m_Q \rightarrow \infty} \epsilon_{m_Q} = 0$ ) of the original Problem (1).

### A. Key Assumptions on Step Sizes

To state the convergence results, we need to lay down some assumptions on the sequence of step sizes:

*Assumption 2. (Assumptions on step size:)*

The step-sizes  $\{\alpha_t\}$ ,  $\{\beta_t\}$ ,  $\{\eta_t\}$  and  $\{\gamma_t\}$  are deterministic and non-increasing, and satisfy:

- 1)  $\alpha_t \rightarrow 0$ ,  $\frac{1}{\alpha_t} \leq O(t^\kappa)$  for some  $\kappa \in (0, 1)$ ,  $\sum_t \alpha_t t^{-1} < \infty$ ,  $\sum_t (\alpha_t)^2 < \infty$ .
- 2)  $\beta_t \rightarrow 0$ ,  $\sum_t \beta_t = \infty$ ,  $\sum_t (\beta_t)^2 < \infty$ ,  $\lim_{t \rightarrow \infty} \beta_t \alpha_t^{-1} = 0$ ,  $\sum_t \alpha_t \beta_t \log t < \infty$ .
- 3)  $\eta_t \rightarrow 0$ ,  $\gamma_t \rightarrow 0$ ,  $\sum_t \eta_t = \infty$ ,  $\sum_t \gamma_t = \infty$ .
- 4)  $\sum_t \alpha_t (1 - \gamma_t) \frac{1}{\gamma_{n_t}^{1/2}} < \infty$ ,  $\sum_t \alpha_t \gamma_{n_t}^{1/2} \eta_{n_t}^{-1/2} < \infty$ ,  $\sum_t m_Q \alpha_t \gamma_{n_t}^{1/2} \eta_{n_t}^{1/2} t^{0.215} < \infty$ ,  $\sum_t m_Q \alpha_t \eta_{n_t} t^{-0.57} < \infty$ , and  $\sum_t m_Q \alpha_t \eta_{n_t} \beta_{n_t} t^{0.86} < \infty$ , where  $n_t = t - t^{0.43}$ .

Please note that Assumptions 2.1)-2.3) are common in the works [47], [7], and [26]. On the other hand, Assumption 2.4) is newly added to ensure that the critic module converges fast enough for asymptotic consistency in section IV-C to be satisfied. Although Assumption 2.4) seems complicated, it is crucial. To make the step size assumptions as intuitive as possible, we set the step size  $\alpha_t = O(m_Q^{-1/2} t^{-\kappa_1})$ ,  $\beta_t = O(m_Q^{-1/2} t^{-\kappa_2})$ ,  $\eta_t = O(m_Q^{-1/2} t^{-\kappa_3})$ , and  $\gamma_t = O(t^{-\kappa_4})$ , and then the Assumption 2 can be satisfied when  $\kappa_i, i = 1, \dots, 4$  lies in the following region

$$\begin{cases} 1 > 2\kappa_2 - 1 > \kappa_1 > 0.43 > \kappa_4 > 0, \\ \min\{0.5\kappa_1 + 0.5\kappa_2 + 0.5\kappa_3 - 0.5, \kappa_1 + \kappa_3\} > 0.43, \\ \kappa_1 + 0.5\kappa_4 - 0.5\kappa_3 > 1, \\ \kappa_1 + 0.5\kappa_3 + 0.5\kappa_4 > 1.215. \end{cases}$$

In practice, we can choose  $\kappa_1, \kappa_2, \kappa_3, \kappa_4$  in the regions  $(0.5, 1)$ ,  $(0.5 + 0.5\kappa_1, 1)$ ,  $(\max\{0.43 - \kappa_1, 1.92 - \kappa_1 - \kappa_2\}, 1)$ , and  $(\max\{2 + \kappa_3 - 2\kappa_1, 2.43 - 2\kappa_1 - \kappa_3\}, 0.43)$  in turn to ensure this set of inequalities satisfied, e.g.  $\kappa_1 = 0.9, \kappa_2 = 0.96, \kappa_3 = 0.21$ , and  $\kappa_4 = 0.42$  is a point in this region.

*Remark 2. (Suggestion for step size selection in practice)*

The above step size region is chosen to facilitate rigorous convergence proof, considering that it is very difficult to bound various convergence errors due to the single-loop design and observation reuse to reduce the interaction cost and complexity. As such, the step size conditions in Assumption 2 are sufficient but not necessary for convergence. The actual step size region used in practice can be wider. In fact, we can appropriately choose larger step size parameters  $\kappa_1, \kappa_2, \kappa_3, \kappa_4$  with slower decreasing speed for the step sizes in practice, because faster initial convergence speed is generally preferred. In the experiments, we follow the general step-size rule in Assumption 2 but slightly relax the conditions to achieve a good convergence speed. The exact values of the step sizes are given in the simulation section for each application example.

### B. Convergence of the Critic Module

Recalling that the task of the critic module is to approximate the surrogate Q functions  $\{\hat{Q}_i^{\pi_{\theta_t}}\}_{i=0, \dots, I}$  using DNNs  $\{f(\bar{\omega}^i)\}_{i=0, \dots, I}$ , we derive the estimated error  $\epsilon_{\text{cri}}(t) \triangleq$

$|\mathbb{E}_{p_t}[f(\bar{\omega}_t^i) | \bar{\omega}_{t-1}^i] - \hat{Q}_i^{\pi_{\theta_t}}|, \forall i$  in this section. For notation simplicity, we denote  $\mathbb{E}_{p_t}[\cdot | \bar{\omega}_{t-1}^i]$  as  $\mathbb{E}[\cdot]$ , and the same abbreviation also applies to other parameters and vectors below, when no confusion arises.

1) *Auxiliary Functions:* Before formally presenting the convergence result, we first define an auxiliary function class  $\hat{\mathcal{F}}$  for the intractable convergence analysis for DNNs, as with [20] and [41]:

*Definition 1. (Local Linearization Function Class)*

For each critic DNN function  $f$ , we define a function class:

$$\hat{\mathcal{F}} = \left\{ \hat{f}(\omega) = f(\omega_0) + \langle \nabla_{\omega} f(\omega_0), \omega - \omega_0 \rangle : \omega \in \mathbb{B}(\omega_0, R_{\omega}) \right\},$$

where  $\omega_0$  is the randomly initialized parameter, and we denote by  $\langle \cdot, \cdot \rangle$  the inner product. Then, based on  $\nabla_{\omega} f(\omega_0)$ , we define a square matrix similar to [42]:

$$\mathbf{A}_{\theta_t} \triangleq \mathbb{E}_{p_t} \left[ \nabla_{\omega} f(\omega_0; \mathbf{s}_t, \mathbf{a}_t) \left( \nabla_{\omega} f(\omega_0; \mathbf{s}_t, \mathbf{a}_t) - \nabla_{\omega} f(\omega_0; \mathbf{s}_{t+1}, \mathbf{a}'_{t+1}) \right)^{\top} \right],$$

$\hat{\mathcal{F}}$  is a sufficiently rich function class for a large critic network width  $m_Q$  and radius  $R_{\omega}$ . It's worth noting that function  $\hat{f} \in \hat{\mathcal{F}}$  can be seen as a local linearization of the critic DNN function  $f$  and satisfies a nice property

$$\hat{f}(\omega_a) - \hat{f}(\omega_b) = \langle \nabla_{\omega} f(\omega_0), \omega_a - \omega_b \rangle. \quad (23)$$

By introducing auxiliary function  $\hat{f}$ , the error  $\epsilon_{\text{cri}}(t)$  is decomposed into two parts, i.e., the local linearization error between  $f$  and  $\hat{f}$  in (42) and the bias  $|\mathbb{E}[\hat{f}(\bar{\omega}_t^i)] - \hat{Q}_i^{\pi_{\theta_t}}|, \forall i$ . Specifically, we give the linearization error in Appendix A and focus on deriving  $|\mathbb{E}[\hat{f}(\bar{\omega}_t^i)] - \hat{Q}_i^{\pi_{\theta_t}}|, \forall i$ , in the following.

2) *Assumptions on the Targets:* For the surrogate Q functions  $\{\hat{Q}_i^{\pi_{\theta_t}}, \forall i\}$ , we have the following standard assumptions:

*Assumption 3. (Assumptions on  $\{\hat{Q}_i^{\pi_{\theta_t}}\}_{i=0, \dots, I}$ )*

1) The inequality  $\omega^{\top} \mathbf{A}_{\theta_t} \omega > 0, \forall t$  holds for any  $\omega$ , which further implies that there is a lower bound  $\varsigma > 0$ , such that

$$\lambda_{\min}(\mathbf{A}_{\theta_t} + \mathbf{A}_{\theta_t}^{\top}) \geq \varsigma$$

holds uniformly for all  $\theta_t \in \Theta$ , where  $\lambda_{\min}(\cdot)$  represents the smallest eigenvalue.

2)  $\hat{\mathcal{F}}$  is closed under the Bellman operator, and there is a point  $\bar{\omega}_t^i$  in the constraint set  $\Omega_i = \mathbb{B}(\omega_0^i, R_{\omega})$  such that  $\hat{f}(\bar{\omega}_t^i) = \mathcal{T}_{\pi_{\theta_t}} \hat{f}(\bar{\omega}_t^i) = \hat{Q}_i^{\pi_{\theta_t}}, \forall i$  for any  $\pi_{\theta_t}$ .

Note that Assumption 3.1 is standard as in [42] to guarantee the existence and uniqueness of the problem (8). Assumption 3.2 is a regularity condition commonly used in [20], [48] and [49], which states that the representation power of  $\hat{\mathcal{F}}$  is sufficiently rich to represent  $\hat{Q}_i^{\pi_{\theta_t}}, \forall i$ . Based Assumption 3.2 and the property (23), it is obtained that,  $\forall i$ ,

$$\begin{aligned} & |\mathbb{E}[\hat{f}(\bar{\omega}_t^i)] - \hat{Q}_i^{\pi_{\theta_t}}| \\ & \leq \|\nabla_{\omega} f(\omega_0)\|_2 \cdot \|\mathbb{E}[\bar{\omega}_t^i] - \bar{\omega}_t^i\|_2, \forall i. \end{aligned} \quad (24)$$

3) *Auxiliary Parameters:* For (24),  $\|\nabla_{\omega} f(\omega_0)\|$  can be easily bounded according to Appendix A, however, it is still non-trivial to derive  $\|\mathbb{E}[\bar{\omega}_t^i] - \bar{\omega}_t^i\|$ . In the single-loop framework, the critic module is only allowed to update DNNs once or for a few finite times in each iteration, to "learn" the

constantly changing targets  $\{\hat{Q}_i^{\pi_{\theta_t}}\}_{i=0,\dots,I}$ . Thus, the error between  $\mathbb{E}[\bar{\omega}_t^i]$  and  $\dot{\omega}_t^i$  is introduced both by the finite-time critic update and by the change of policy  $\pi_{\theta_t}$ .

To separate the two coupled errors, we define two auxiliary parameters  $\{\mathbf{m}_t^i, \bar{\mathbf{m}}_t^i, \forall i\}$ . The two auxiliary parameters are updated by the same rules as  $\{\omega^i, \bar{\omega}^i, \forall i\}$  but use the local linearization function  $\hat{f}$  and auxiliary observations  $\tilde{\varepsilon}_t = \{\tilde{\mathbf{s}}_t, \tilde{\mathbf{a}}_t, \{C_i(\tilde{\mathbf{s}}_t, \tilde{\mathbf{a}}_t)\}_{i=0,\dots,I}, \tilde{\mathbf{s}}_{t+1}\}$ , where  $\tilde{\varepsilon}_t$  is sampled by  $\pi_{\theta_t}$  before the  $n_t$ -th iteration and by the fixed policy  $\pi_{\theta_{n_t+1}}$  after the  $(n_t + 1)$ -th iteration, and where we set  $n_t = t - t^{\kappa_5}$ ,  $\kappa_5 \in (0, 1)$ . Please refer to (44)-(46) for details. Based on this, we can decompose the convergence error into the error caused by the change of policy and the error caused by finite critic updates. Thus, we have that

$$\|\mathbb{E}[\bar{\omega}_t^i] - \dot{\omega}_t^i\| \leq \|\mathbb{E}[\bar{\omega}_t^i] - \mathbb{E}[\bar{\mathbf{m}}_t^i]\| + \|\mathbb{E}[\bar{\mathbf{m}}_t^i] - \dot{\omega}_t^i\|, \quad (25)$$

,  $\forall i$ , where the first term presents the distance between the fixed policy update trajectory and the unfixed policy update trajectory, and the second term characterizes the error induced by finite-time critic updates. We bounded them in Appendix B, respectively.

4) *The Convergence Rate of Critic Module:* Finally, we obtain the convergence rate of the critic module:

*Lemma 1. (Convergence rate of the Critic Module)*

Suppose Assumption 1 and Assumption 3 hold, the width of critic DNNs is  $m_Q$ , and the radius  $R_\omega$  of the parameter constraint set  $\Omega = \mathbb{B}(\omega_0^i, R_\omega)$  is specifically set to  $R_\omega = a_0 m_Q^{-1/2} L^{-4/9}$ . Then, it holds that

$$\begin{aligned} \epsilon_{\text{cri}}(t) &\triangleq \left| \mathbb{E}[f(\bar{\omega}_t^i; \mathbf{s}, \mathbf{a})] - \hat{Q}_i^{\pi_{\theta_t}}(\mathbf{s}, \mathbf{a}) \right| \\ &\leq O\left(\epsilon_{m_Q} + \frac{(1 - \gamma_t)^{t^{\kappa_5}/2}}{\gamma_t^{1/2}} + m_Q \gamma_{n_t}^{1/2} \eta_{n_t}^{1/2} t^{0.215} \right. \\ &\quad \left. + m_Q \eta_{n_t} t^{-0.57} + \frac{\gamma_{n_t}^{1/2}}{\eta_{n_t}^{1/2}} + m_Q \eta_{n_t} \beta_{n_t} t^{0.86}\right), \end{aligned}$$

with almost probability 1, where  $\epsilon_{m_Q} \triangleq O(m_Q^{-1/6} \sqrt{\log m_Q})$  and  $\lim_{m_Q \rightarrow \infty} \epsilon_{m_Q} = 0$ .

Remark that we choose this particular radius  $R_\omega = a_0 m_Q^{-1/2} L^{-4/9}$  following the same setup as [41] just for tractable convergence analysis. Although  $R_\omega$  in Lemma 1 seems small but is in fact sufficiently large to enable a powerful representation capability for the critic DNNs to fit the training data because the weights are randomly initialized (per entry) around  $m_Q^{-1/2}$  for  $m_Q$  being large [38]. In particular, [38] states that with the DNN defined in II-B, the SGD method can find global minima in the neighborhood  $\mathbb{B}(\omega, R_\omega)$  on the training objective of overparameterized DNNs, as long as  $R_\omega \geq O(m_Q^{-1/2})$ .

According to Assumption 2 and

$$\sum_{t=0}^{\infty} \alpha_t |f(\bar{\omega}_t^i; \mathbf{s}, \mathbf{a}) - \hat{Q}_i^{\pi_{\theta_t}}(\mathbf{s}, \mathbf{a})| < \infty, \quad (26)$$

which is required in the proof of asymptotic consistency of surrogate functions below (Please refer to (70) for details). More intuitively, if we set the step size  $\alpha_t = O(m_Q^{-1/2} t^{-\kappa_1})$ ,

we can further have

$$\epsilon_{\text{cri}}(t) \leq O(t^{\kappa_1 - 1}). \quad (27)$$

### C. Consistency of Surrogate Functions

Although the single-loop design and the observation reuse make  $\hat{J}_i^t$  and  $\hat{\mathbf{g}}_i^t$  biased estimation, we manage to prove that  $\hat{J}_i^t$  and  $\hat{\mathbf{g}}_i^t$  used to construct the surrogate functions satisfy asymptotic consistency, which is a key to establish the global convergence:

*Lemma 2. (Asymptotic consistency of surrogate functions)*

Suppose that Assumptions 1-3 are satisfied, and the width of critic DNNs is  $m_Q$ . Then, for all  $i \in \{0, 1, \dots, I\}$ , we have

$$\lim_{t \rightarrow \infty} |\hat{J}_i^t - J_i(\theta_t)| = 0, \quad (28)$$

$$\lim_{t \rightarrow \infty} \|\hat{\mathbf{g}}_i^t - \nabla J_i(\theta_t)\|_2 \leq \epsilon_{m_Q}, \quad (29)$$

where  $\epsilon_{m_Q} \triangleq O(m_Q^{-1/6} \sqrt{\log m_Q})$  and  $\lim_{m_Q \rightarrow \infty} \epsilon_{m_Q} = 0$ .

*Proof:* Since we adopt recursive operations to obtain  $\hat{J}_i^t$  and  $\hat{\mathbf{g}}_i^t$  in (15) and (16), the proof can be completed as long as some key conditions are proved to be satisfied, i.e.,  $\sum_{t=0}^{\infty} \alpha_t |\mathbb{E}[\hat{J}_i^t] - J_i(\theta_t)| < \infty$  and  $\sum_{t=0}^{\infty} \alpha_t \|\mathbb{E}[\hat{\mathbf{g}}_i^t] - \nabla J_i(\theta_t)\|_2 < \infty$  according to Lemma 5. Please refer to Appendix C for details. ■

### D. Convergence of the Actor Module

This subsection proves that the proposed SLDAC algorithm converges to a KKT point (up to an error of  $\epsilon_{m_Q}$  with  $\lim_{m_Q \rightarrow \infty} \epsilon_{m_Q} = 0$ ) of the original Problem (1). We begin with the definition of KKT solutions of the original problem.

*Definition 2. (KKT solution of the original problem)*

A solution  $\theta^*$  is called a KKT solution of the original problem, if there exist Lagrange multipliers  $\lambda = [\lambda_1, \dots, \lambda_I]^T \succeq \mathbf{0}$ , such that the following conditions are satisfied:

$$\mathbf{g}_0(\theta^*) + \sum_i \lambda_i \mathbf{g}_i(\theta^*) = \mathbf{0} \quad (30)$$

$$J_i(\theta^*) \leq 0, i = 1, \dots, I, \quad (31)$$

$$\lambda_i J_i(\theta^*) = 0, i = 1, \dots, I. \quad (32)$$

Moreover, considering a subsequence  $\{\theta_{t_j}\}_{j=1}^{\infty}$  converging to a limiting point  $\theta^*$ , there exist converged surrogate functions  $\hat{J}_i(\theta), \forall i$  such that

$$\lim_{j \rightarrow \infty} \hat{J}_i^{t_j}(\theta) = \hat{J}_i(\theta), \forall \theta \in \Theta, \quad (33)$$

where

$$|\hat{J}_i(\theta^*) - J_i(\theta^*)| = 0, \quad (34)$$

$$\|\nabla \hat{J}_i(\theta^*) - \nabla J_i(\theta^*)\|_2 = 0. \quad (35)$$

Then, with Lemma 2 and Assumptions 1 - 3, we are ready to prove the main convergence theorem:

*Theorem 1. (Global Convergence of Algorithm 1:)*

Suppose Assumptions 1 - 3 are satisfied, the initial point  $\theta_0$  is feasible, i.e.,  $\max_{i \in \{1, \dots, I\}} J_i(\theta_0) \leq 0$ , and the number of data samples is set to  $T_t = O(\log t)$ . Denote  $\{\theta_t\}_{t=1}^{\infty}$  as the iterates generated by Algorithm 1 with a sufficiently small initial step size  $\beta_0$ . Then, every limiting point  $\theta^*$  of  $\{\theta_t\}_{t=1}^{\infty}$  satisfying



the Slater condition satisfies the KKT conditions in (30), (31), and (32) up to an error of  $\epsilon_{m_Q} \triangleq O(m_Q^{-1/6} \sqrt{\log m_Q})$ , i.e.,

$$\|g_0(\boldsymbol{\theta}^*) + \sum_i \lambda_i g_i(\boldsymbol{\theta}^*)\|_2 \leq \epsilon_{m_Q} \quad (36)$$

$$J_i(\boldsymbol{\theta}^*) \leq \epsilon_{m_Q}, i = 1, \dots, I, \quad (37)$$

$$\lambda_i J_i(\boldsymbol{\theta}^*) \leq \epsilon_{m_Q}, i = 1, \dots, I. \quad (38)$$

where  $\lim_{m_Q \rightarrow \infty} \epsilon_{m_Q} = 0$ .

According to this theorem, the reader can appropriately take  $m_Q$  that satisfies the performance requirements. The key challenges in the convergence analysis lie in the proof of Lemma 1-3. Once Lemma 1-3 are proved in this paper, Theorem 1 follows from the similar analyses in our previous work [50] and [7], and we omit it due to the space limit.

Finally, we discuss the convergence behavior of Algorithm 1 with an infeasible initial point. In this case, it follows from the same analysis in Appendix B of our related work [7] that Algorithm 1 either converges to a KKT point of Problem (1), or converges to the following *undesired set*:

$$\overline{\Theta}_C^* = \{\boldsymbol{\theta} : J(\boldsymbol{\theta}) > 0, \boldsymbol{\theta} \in \Theta_C^*\}, \quad (39)$$

where  $\Theta_C^*$  is the set of stationary points of the following constraint minimization problem:

$$\min_{\boldsymbol{\theta} \in \Theta} J(\boldsymbol{\theta}) \triangleq \max_{i \in \{1, \dots, I\}} J_i(\boldsymbol{\theta}) \quad (40)$$

Thanks to the proposed feasible update (21), Algorithm 1 may still converge to a KKT point (up to an error of  $\epsilon_{m_Q}$ ) of Problem (1) even with an infeasible initial point, as long as the initial point is not close to an undesired point  $\boldsymbol{\theta}_C^* \in \overline{\Theta}_C^*$  such that the algorithm gets stuck in this undesired point. In practice, if we generate multiple random initial points, it is likely that one of the iterates starting from these random initializers will not get stuck in undesired points, and the algorithm will converge to a KKT point (up to an error of  $\epsilon_{m_Q}$ ) of Problem (1).

## V. SIMULATION RESULTS

In this section, we apply the proposed SLDAC to solve the three typical CRL application problems in Section II-A. We maintain the lengths of observation storage  $T = 1000, 30000, 500$  and interact with the environment to obtain  $B = 100, 10000, 100$  new observations at each iteration in Example 1, Example 2, and Example 3, respectively. The policy mean network and the standard deviation network, as well as all critic networks of all algorithms are parameterized by the fully-connected DNN defined in Section II-B, where the number of hidden layers is 2 and the width is 128. In addition, we updated the critic parameters  $\omega_i, \forall i$  using a fixed step size  $\eta_t = 0.001$ , and then fine tune the other step sizes  $\{\alpha_t, \beta_t, \gamma_t\}$  to achieve a good convergence speed. Please note that although we appropriately relax some conditions assumed for rigorous convergence proof, i.e.,  $T_t = O(\log t)$ ,  $m_Q$  is sufficiently large and the requirements for step sizes given in Assumption 2, the algorithm can still have a good convergence behavior.

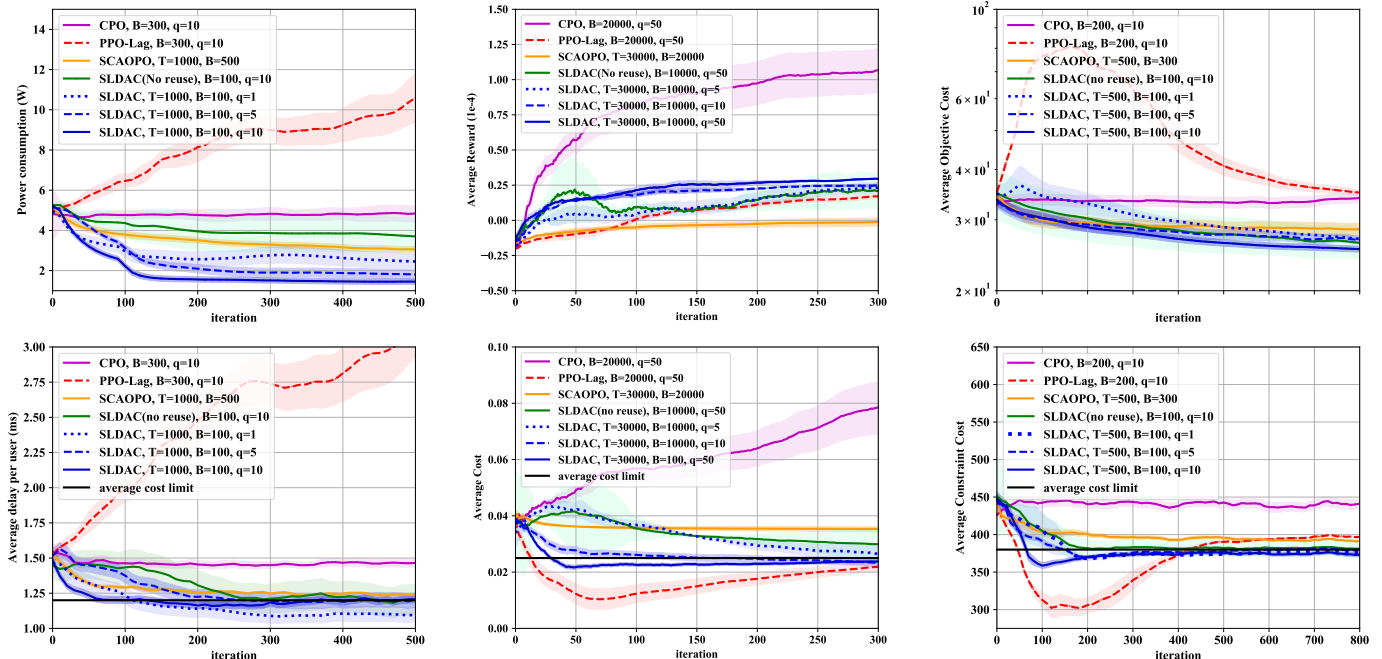
We adopt the advanced Actor-only algorithm SCAOPO [7] and the classical two-loop DAC algorithms, PPO-Lag [17] and CPO [23], as baselines to evaluate the performance of dual critic DNNs and the CSSCA-based policy optimization of the

proposed SLDAC, respectively. To demonstrate the effect of the single-loop design, we simulate the SLDAC with  $q = 1, 5$ , and 10 critic updates at each iteration, respectively. Since the two-loop DAC requires the critic module to constantly update until the Q-values are accurately estimated, which is impractical, so we did not directly show it in the simulation results. However, the proposed algorithm with a larger  $q$ , i.e.,  $q = 10$  in Example 1 and 3, and  $q = 50$  in Example 2, can be viewed as a practical implementation of the two-loop DAC. We also simulate the SLDAC without storing and reusing previous data samples to demonstrate the benefit of reusing old experiences. Moreover, the results of each algorithm are averaged across 10 random seeds.

### A. Delay-Constrained Power Control for Downlink MU-MIMO

Following the same standard setup implemented as [7], we adopt a geometry-based channel model  $\mathbf{h}_k = \sum_{i=1}^{N_p} \bar{\alpha}_{k,i} \mathbf{a}(\psi_{k,i})$  for simulation, where  $\mathbf{a}(\psi_{k,i}) = [1, e^{j\pi \sin(\psi)}, \dots, e^{j(N_t-1)\pi \sin(\psi)}]^\top$  is the half-wavelength spaced uniform linear array (ULA) response vector,  $N_p$  denotes the number of scattering path, and  $\psi_{k,i}$  denotes the  $i$ -th angle of departure (AoD). We assume that  $\varphi_{k,i}$ 's with an angular spread  $\sigma_{AS} = 5$  and  $\bar{\alpha}_{k,i} \sim \mathcal{CN}(0, \bar{\sigma}_{k,i}^2)$  are Laplacian distributed,  $\bar{\sigma}_{k,i}^2$ 's follow an exponential distribution and are normalized such that  $\sum_{i=1}^{N_p} \bar{\sigma}_{k,i}^2 = g_k$ , where  $g_k$  represents the path gain of the  $k$ -th user. Specially, we uniformly generate the path gains  $g_k$ 's from -10 dB to 10 dB and set  $N_p = 4$  for each user. In addition, the bandwidth  $\bar{B} = 10$  MHz, the duration of one time slot  $\bar{\tau} = 1$  ms, the noise power density -100 dBm/Hz, and the arrival data rate  $A_k, \forall k$  are uniformly distributed over  $[0, 20]$  Mbit/s. The constants in the surrogate problems are  $\zeta_k = 1, \forall k$ . In this case, we choose the step sizes as  $\alpha_t = \frac{1}{t^{0.6}}, \beta_t = \frac{1}{t^{0.7}},$  and  $\gamma_t = \frac{1}{t^{0.3}}.$

In Fig. 3, we plot the average power consumption and the average delay per user when the number of transmitting antennas  $N_t = 8$  and the number of receiving antennas for users  $K = 4$ . Compared with the classical DAC algorithms PPO-Lag and CPO, the proposed SLDAC can significantly reduce power consumption while meeting the delay constraint regardless of whether data reuse is adopted, which reveals the benefit of the guarantee of convergence to a KKT point. In terms of SCAOPO, its convergence rate depends heavily on the number of observations, because its policy gradient is calculated using MC methods. Even though we feed the SCAOPO more newly added observations at each iteration, i.e.,  $B = 500$ , the proposed SLDAC still demonstrates comparable or superior performance to the SCAOPO. For the proposed SLDAC, it can be seen that the performance at  $q = 1$  is already good, the performance at  $q = 5$  is almost the same as the performance at  $q = 10$ , and obviously, there is no need to continue increasing  $q$ . By comparing the simulation results for  $q = 5$  and  $q = 10$ , it is clear that the proposed algorithm with a relatively small  $q$  requires much fewer interactions with the environment to achieve the same convergence performance, which implies that the single-loop framework can indeed reduce the interaction cost compared to the two-loop framework. In addition, the SLDAC with observation reuse can attain better performance than that without observation because the old observations



(a) Delay-constrained power control for downlink MU-MIMO. (b) Autonomous vehicle transport with safety assurance. (c) Constrained linear-quadratic regulator.

Figure 3. The first and second rows of images respectively show the learning curves of average rewards and costs in three typical scenarios, respectively, where the lines show the average performance of the algorithms, and the shade regions indicate half the standard deviations.

generated from the old policy also contain information that can be exploited.

### B. Robot Navigation with Safety Assurance

By choosing the step sizes  $\alpha_t = \frac{1}{t^{0.55}}$ ,  $\beta_t = \frac{1}{t^{0.75}}$ , and  $\gamma_t = \frac{1}{t^{0.4}}$  and setting the average cost limit  $c_1 = 0.025$  and the surrogate problems are  $\zeta_i = 1, \forall i$ , we obtain the simulation results shown in Fig. 3b. It can be seen that CPO failed due to significant approximation errors in this complex scenario. Although PPO-Lag was able to meet the constraints, the average reward obtained is relatively low due to its simple stochastic gradient descent-based policy update method. In terms of SCAOPO, it can only receive a negative average reward because the MC method has a large error in estimating Q in this scenario. In contrast, the proposed SLDAC can receive significantly higher average reward while meeting the average cost limit regardless of whether data reuse is adopted, which reveals the benefit of the guarantee of convergence to a KKT point. Moreover, due to the special single-loop framework design, the SLDAC algorithm has a good performance even with a relatively small  $q$  than that in baseline algorithms.

### C. Constrained Linear-Quadratic Regulator

Similar to [51] and [7], we set the state dimension  $n_s = 15$ , action dimension  $n_a = 4$ , the average constraint cost limit  $c_1 = 380$ , and the constants in the surrogate problems  $\zeta_i = 10, \forall i$ . Then, by choosing the step sizes  $\alpha_t = \frac{1}{t^{0.6}}$ ,  $\beta_t = \frac{1}{t^{0.8}}$ , and  $\gamma_t = \frac{1}{t^{0.27}}$ , we obtain the simulation results shown in Fig. 3c. As it can be seen from the figures, we obtain a similar behavior as in the other two scenario that the proposed SLDAC with appropriately chosen  $q$  provides the best performance.

## VI. CONCLUSION

In this work, we proposed a novel SLDAC algorithm, which is the first single-loop DAC variant to solve general CMDPs with guaranteed convergence. Compared with existing algorithms, the proposed SLDAC considers more requirements in many realistic domains. Specifically, the CSSCA-based policy optimization method is used to better handle the non-convex stochastic objective and constraints, and the single-loop framework and observation reuse are adopted to reduce the computational complexity and interaction cost. Under some technical conditions, we provide the finite-time convergence rate of critic DNNs and the asymptotic consistency of estimated surrogate functions. Finally, we prove that the SLDAC converges to a KKT point of the original problem almost surely. Simulation results show that the proposed SLDAC can achieve a better overall performance compared to baselines with much lower interaction cost.

## APPENDIX A

### TECHNICAL BOUNDS ABOUT DNNs

In this section, we show some bounds for the critic DNNs and the error introduced by local linearization. Recalling that  $m_Q$  represents the width of critic DNNs,  $L$  stands for the depth of the critic DNNs, and  $R_\omega$  denotes the radius of the constraint set  $\Omega = \mathbb{B}(\omega_0^i, R_\omega)$  for the parameter  $\omega$ , we restate a useful lemma from recent studies of overparameterized DNNs [41, Lemma 6.4], [39, Lemma B.3], and [38, Theorem 5].

*Lemma 3. (Technical Bounds about DNN:)*

Let  $\sigma \in (0, 1)$ ,  $d$  and  $\{a_i\}_{i=0,1,\dots}$  denote some universal constants that are independent of problem parameters throughout this paper. Then, for any  $\sigma > 0$ , if  $a_1 d^{3/2} L^{-1} m_Q^{-3/4} \leq R_\omega \leq a_2 L^{-6} (\log m_Q)^{-3}$  and  $m_Q \geq$

$a_3 \max\{dL^2 \log(m_Q/\sigma), R_\omega^{-4/3} L^{-8/3} \log(m_Q/(R_\omega \sigma))\}$  are satisfied, it holds that the difference between the  $f(\omega)$  and its local linearization  $\hat{f}(\omega)$

$$|f(\omega; \mathbf{s}, \mathbf{a}) - \hat{f}(\omega; \mathbf{s}, \mathbf{a})| \leq a_4 R_\omega^{4/3} L^4 \sqrt{m_Q \log m_Q} + a_5 R_\omega^2 L^5, \\ \forall \phi(\mathbf{s}, \mathbf{a}) \in \mathbb{R}^d, \text{ with probability at least } 1 - \sigma - \exp\{-a_6 m_Q R_\omega^{2/3} L\}. \text{ Moreover, the gradient of the DNN is also bounded as } \|\nabla_\omega f(\omega; \mathbf{s}, \mathbf{a})\|_2 \leq a_7 m_Q^{1/2} \text{ with probability at least } 1 - L^2 \exp\{-a_8 m_Q R_\omega^{2/3} L\}.$$

Specially, we set all critic parameters to have the same initial values, i.e.,  $\omega_0^i = \bar{\omega}_0^i = \mathbf{m}_0^i = \bar{\mathbf{m}}_0^i = \omega_0, \forall i$ , and generate the initial parameter  $\omega_0$  from  $\mathcal{N}(0, 1/m_Q^2)$ . Then, it holds that  $\|\omega\|_2 \leq a_9 m_Q^{1/2}$ .

## APPENDIX B PROOF OF LEMMA 1

For simplicity, we omit the superscript  $i$  when no confusion arises in this section. By introducing the auxiliary function class  $\mathcal{F}$ , the estimated error in the critic module can be divided as follows

$$\underbrace{|\mathbb{E}[f(\bar{\omega}_t)] - \hat{Q}^{\pi_{\theta_t}}|}_{\text{bias}_1} \leq |\mathbb{E}[f(\bar{\omega}_t) - \mathbb{E}[\hat{f}(\bar{\omega}_t)]]| + |\mathbb{E}[\hat{f}(\bar{\omega}_t)] - \hat{f}(\dot{\omega}_t)|, \quad (41)$$

The first term in (41), bias 1, characterizes how far  $f$  deviates from its local linearization  $\hat{f}$ . According to Appendix A, if we specially set the radius  $R_\omega = a_0 m_Q^{-1/2}$ , and assume that  $m_Q$  is sufficiently large, then it holds that

$$\text{bia}_1 \triangleq \epsilon_{m_Q} \leq O(m_Q^{-1/6} \sqrt{\log m_Q}). \quad (42)$$

For the second term (41), since  $\hat{f}$  is a linear function, we have

$$|\mathbb{E}[\hat{f}(\bar{\omega}_t)] - \hat{Q}^{\pi_{\theta_t}}| \leq \|\nabla_\omega f(\omega_0)\|_2 \cdot \|\mathbb{E}[\bar{\omega}_t] - \dot{\omega}_t\|_2, \quad (43)$$

where recall that  $\|\nabla_\omega f(\omega; \mathbf{s}, \mathbf{a})\|_2 \leq a_7 m_Q^{1/2}$  is given in Appendix A. Then, we analysis the error  $\|\mathbb{E}[\bar{\omega}_t] - \dot{\omega}_t\|_2$ .

We further introduce two auxiliary parameters  $\{\mathbf{m}, \bar{\mathbf{m}}, \forall i\}$ , whose the update process can be formulated as

$$\mathbf{m}_t = \Pi_{\Omega_i}(\mathbf{m}_{t-1} - \eta_t \mathbf{M}^{\mathbf{m}_t}), \forall i, \quad (44)$$

$$\bar{\mathbf{m}}_t = (1 - \gamma_t) \bar{\mathbf{m}}_{t-1} + \gamma_t \mathbf{m}_t. \quad (45)$$

where recalling  $\Delta^{\omega_{t-1}}$  defined in (12), the stochastic gradient term  $\mathbf{M}^{\mathbf{m}_{t-1}}$  is defined as

$$\mathbf{M}^{\mathbf{m}_{t-1}} = \left( \hat{f}(\mathbf{m}_{t-1}; \tilde{\mathbf{s}}_t, \tilde{\mathbf{a}}_t) - (C'_i(\tilde{\mathbf{s}}_t, \tilde{\mathbf{a}}_t) - \hat{J}_i^{t-1} + \hat{f}(\mathbf{m}_{t-1}; \tilde{\mathbf{s}}_{t+1}, \tilde{\mathbf{a}}'_{t+1})) \right) \nabla_\omega f(\mathbf{m}_0; \tilde{\mathbf{s}}_t, \tilde{\mathbf{a}}_t), \quad (46)$$

where  $\tilde{\mathbf{a}}'_{t+1}$  is the action chosen by current policy at the next state  $\tilde{\mathbf{s}}_{t+1}$ . Based on the auxiliary parameters, we divided  $\|\mathbb{E}[\bar{\omega}_t] - \dot{\omega}_t\|_2$  into two parts

$$\|\mathbb{E}[\bar{\omega}_t] - \dot{\omega}_t\|_2 \leq \underbrace{\|\mathbb{E}[\bar{\mathbf{m}}_t] - \dot{\omega}_t\|_2}_{\text{bias}_2} + \underbrace{\|\mathbb{E}[\bar{\omega}_t] - \mathbb{E}[\bar{\mathbf{m}}_t]\|_2}_{\text{bias}_3}, \quad (47)$$

where bias 2 characterizes the error induced by finite-time critic updates and bias 3 presents the distance between the fixed policy update trajectory and the unfixed policy update trajectory. We derive the two in the following, respectively.

a) *bias 2*: According to (45), we have

$$\bar{\mathbf{m}}_t = \sum_{t'=0}^t \prod_{j=t'+1}^t (1 - \gamma_j) \gamma_{t'} \mathbf{m}_{t'}, \forall i, \quad (48)$$

Noting that  $\sum_{t'=0}^t \prod_{j=t'+1}^t (1 - \gamma_j) \gamma_{t'} = 1$ , we can obtain the following derivation according to the Jensen's inequality:

$$\begin{aligned} \|\mathbb{E}[\bar{\mathbf{m}}_t] - \dot{\omega}_t\|_2^2 &\leq \sum_{t'=0}^t \prod_{j=t'+1}^t (1 - \gamma_j) \gamma_{t'} \|\mathbb{E}[\mathbf{m}_{t'}] - \dot{\omega}_t\|_2^2 \\ &\leq \sum_{t'=0}^t (1 - \gamma_t)^{t-t'} \gamma_{t'} \|\mathbb{E}[\mathbf{m}_{t'}] - \dot{\omega}_t\|_2^2 \\ &\stackrel{a}{\leq} \sum_{t'=0}^{n_t} (1 - \gamma_t)^{t-t'} \|\mathbb{E}[\mathbf{m}_{t'}] - \dot{\omega}_t\|_2^2 \\ &\quad + \frac{\gamma_{n_t}}{\eta_{n_t}} \sum_{t'=n_t+1}^t \eta_{t'} \|\mathbb{E}[\mathbf{m}_{t'}] - \dot{\omega}_t\|_2^2. \end{aligned} \quad (49)$$

For the first term of (49)-a, since  $\max_{t'=0, \dots, n_t} \|\mathbb{E}[\mathbf{m}_{t'}] - \dot{\omega}_t\|_2^2 \leq R_\omega^2 = O(m_Q^{-1})$ , we can obtain that

$$\sum_{t'=0}^{n_t} (1 - \gamma_t)^{t-t'} \|\mathbb{E}[\mathbf{m}_{t'}] - \dot{\omega}_t\|_2^2 \leq O\left(\frac{(1 - \gamma_t)^{t n_5}}{\gamma_t m_Q}\right). \quad (50)$$

Now, we derive the second term of (49)-a. Recalling the update rule of (44), we have

$$\begin{aligned} \|\mathbb{E}[\mathbf{m}_{t'}] - \dot{\omega}_t\|_2^2 &\leq \|\mathbb{E}[\Pi_{\Omega_i}(\mathbf{m}_{t'} - \eta_{t'} \mathbf{M}^{\mathbf{m}_{t'}})] - \dot{\omega}_t\|_2^2 \\ &\leq -2\eta_{t'} \langle \mathbb{E}_{p_{t'}}[\mathbf{M}^{\mathbf{m}_{t'}}] - \mathbb{E}_{p_{t'}}[\mathbf{M}^{\dot{\omega}_t}], \mathbb{E}[\mathbf{m}_{t'}] - \dot{\omega}_t \rangle \\ &\quad + \|\mathbb{E}[\mathbf{m}_{t'}] - \dot{\omega}_t\|_2^2 + \eta_{t'}^2 \|\mathbb{E}[\mathbf{M}^{\mathbf{m}_{t'}}]\|_2^2. \end{aligned} \quad (51)$$

We first derives the inner product term of (51):

$$\begin{aligned} &\langle \mathbb{E}_{p_{t'}}[\mathbf{M}_i^{\mathbf{m}_{t'}}] - \mathbb{E}_{p_{t'}}[\mathbf{M}_i^{\dot{\omega}_t}], \mathbb{E}[\mathbf{m}_{t'}] - \dot{\omega}_t \rangle \\ &\stackrel{a}{=} (\mathbb{E}[\mathbf{m}_{t'}] - \dot{\omega}_t)^\top \mathbf{A}_{\theta_{t'}} (\mathbb{E}[\mathbf{m}_{t'}] - \dot{\omega}_t) \\ &= \frac{1}{2} (\mathbb{E}[\mathbf{m}_{t'}] - \dot{\omega}_t)^\top (\mathbf{A}_{\theta_{n_{t'}+1}} + \mathbf{A}_{\theta_{n_{t'}+1}}^\top) (\mathbb{E}[\mathbf{m}_{t'}] - \dot{\omega}_t) \\ &\geq \frac{1}{2} \lambda_{\min}(\mathbf{A}_{\theta_{n_{t'}+1}} + \mathbf{A}_{\theta_{n_{t'}+1}}^\top) \|\mathbb{E}[\mathbf{m}_{t'}] - \dot{\omega}_t\|_2^2 \\ &\stackrel{b}{\geq} \frac{\varsigma}{2} \|\mathbb{E}[\mathbf{m}_{t'}] - \dot{\omega}_t\|_2^2, \end{aligned} \quad (52)$$

where (52)-a is according to the linear property (23) and (52)-b follows Assumption 3-2). Then, by Appendix A and the fact that cost (reward) function  $C'_i$  is bounded, we have

$$\|\mathbb{E}[\mathbf{M}^{\mathbf{m}_{t'}}]\|_2 \leq a_{11} m_Q^{1/2}, \quad (53)$$

with probability at least  $1 - L^2 \exp\{-a_8 m_Q R_\omega^{2/3} L\}$ . Further, by substituting (52) and (53) into (51), and rearranging the terms, we can obtain that

$$\begin{aligned} &\|\mathbb{E}[\mathbf{m}_{t'}] - \dot{\omega}_t\|_2^2 \\ &\leq \frac{\|\mathbb{E}[\mathbf{m}_{t'}] - \dot{\omega}_t\|_2^2 - \|\mathbb{E}[\mathbf{m}_{t'+1}] - \dot{\omega}_t\|_2^2}{\eta_{t'} \varsigma} + \frac{a_{11}^2 m_Q \eta_{t'}}{\varsigma}. \end{aligned} \quad (54)$$

Taking summation on both sides of (54), we obtain

$$\begin{aligned} & \sum_{t'=n_t+1}^t \eta_{t'} \|\mathbb{E}[\mathbf{m}_{t'}] - \dot{\boldsymbol{\omega}}_t\|_2^2 \\ & \leq \frac{1}{\varsigma} \|\mathbb{E}[\mathbf{m}_{n_t+1}] - \dot{\boldsymbol{\omega}}_t\|_2^2 + \frac{1}{\varsigma} a_{11}^2 m_Q \eta_{n_t}^2 t^{\kappa_5} \\ & \leq O\left(\frac{1}{\varsigma m_Q} + \frac{a_{11}^2 m_Q \eta_{n_t}^2 t^{\kappa_5}}{\varsigma}\right), \end{aligned} \quad (55)$$

where recall that  $n_t = t - t^{\kappa_5}$ . Finally, plugging (55) into the second term of (49)-a, we can derive that

$$\frac{\gamma_{n_t}}{\eta_{n_t}} \sum_{t'=n_t+1}^t \eta_{t'} \|\mathbb{E}[\mathbf{m}_{t'}] - \dot{\boldsymbol{\omega}}_t\|_2^2 \leq O\left(\frac{\gamma_{n_t} + m_Q^2 \gamma_{n_t} \eta_{n_t}^2 t^{\kappa_5}}{m_Q \eta_{n_t}}\right). \quad (56)$$

Combining (49), (50), and (56), we have

$$\|\mathbb{E}[\bar{\mathbf{m}}_t] - \dot{\boldsymbol{\omega}}_t\|_2^2 \leq O\left(\frac{\gamma_{n_t} + m_Q^2 \gamma_{n_t} \eta_{n_t}^2 t^{\kappa_5}}{m_Q \eta_{n_t}} + \frac{(1 - \gamma_t)^{t^{\kappa_5}}}{m_Q \gamma_t}\right). \quad (57)$$

b) *bias 3*: Together with (13) and (45), we obtain

$$\begin{aligned} & \|\mathbb{E}[\bar{\mathbf{m}}_t] - \mathbb{E}[\bar{\boldsymbol{\omega}}_t]\|_2 \\ & \leq \sum_{t'=n_t+1}^t \prod_{j=t'+1}^t (1 - \gamma_j) \gamma_{t'} \|\mathbb{E}[\mathbf{m}_{t'}] - \mathbb{E}[\boldsymbol{\omega}_{t'}]\|_2 \\ & \leq \sum_{t'=n_t+1}^t (1 - \gamma_t)^{t-t'} \gamma_{t'} e_{n_t}^b = O(e_{n_t}^b \frac{\gamma_{n_t}}{\gamma_t}), \forall i, \end{aligned} \quad (58)$$

where  $e_{n_t}^b = \max_{t'=n_t+1, \dots, t} \{\|\mathbb{E}[\mathbf{m}_{t'}] - \mathbb{E}[\boldsymbol{\omega}_{t'}]\|_2\}$ . According to Assumption 2, we have  $\gamma_{n_t}/\gamma_t < \infty$ , and thus  $O(e_{n_t}^b \gamma_{n_t}/\gamma_t) = O(e_{n_t}^b)$ .

Combining (11) and (44), we have

$$\begin{aligned} & \|\mathbb{E}[\mathbf{m}_{t'}] - \mathbb{E}[\boldsymbol{\omega}_{t'}]\|_2 \\ & \leq \sum_{j=n_t+1}^{t'} \eta_j \|\mathbb{E}[\boldsymbol{\Delta}^{\omega_{j-1}}] - \mathbb{E}[\mathbf{M}^{m_{j-1}}]\|_2 \\ & = \sum_{j=n_t+1}^{t'} \eta_j \left\| \int_{\mathbf{s} \in \mathcal{S}} \mathbf{P}(S_j = d\mathbf{s}) \int_{\mathbf{a} \in \mathcal{A}} \pi_{\theta_j}(d\mathbf{a} | \mathbf{s}) \boldsymbol{\Delta}^{\omega_{j-1}} \right. \\ & \quad \left. - \int_{\tilde{\mathbf{s}} \in \mathcal{S}} \mathbf{P}_{\pi_{\theta_t}} \int_{\tilde{\mathbf{a}} \in \mathcal{A}} \pi_{\theta_t}(d\tilde{\mathbf{a}} | \tilde{\mathbf{s}}) \mathbf{M}^{m_{j-1}} \right\|_2 \\ & \stackrel{a}{\leq} m_Q^{1/2} \sum_{j=n_t+1}^{t'} \eta_j O\left(\left\| \int_{\mathbf{s} \in \mathcal{S}} \mathbf{P}(S_j = d\mathbf{s}) \int_{\mathbf{a} \in \mathcal{A}} \pi_{\theta_j}(d\mathbf{a} | \mathbf{s}) \right. \right. \\ & \quad \left. \left. - \int_{\tilde{\mathbf{s}} \in \mathcal{S}} \mathbf{P}_{\pi_{\theta_t}} \int_{\mathbf{a} \in \mathcal{A}} \pi_{\theta_j}(d\mathbf{a} | \mathbf{s}) \right\|_2 + \left\| \int_{\tilde{\mathbf{s}} \in \mathcal{S}} \mathbf{P}_{\pi_{\theta_t}} \right. \right. \\ & \quad \left. \left. \int_{\mathbf{a} \in \mathcal{A}} \pi_{\theta_j}(d\mathbf{a} | \mathbf{s}) - \int_{\tilde{\mathbf{s}} \in \mathcal{S}} \mathbf{P}_{\pi_{\theta_t}} \int_{\tilde{\mathbf{a}} \in \mathcal{A}} \pi_{\theta_t}(d\tilde{\mathbf{a}} | \tilde{\mathbf{s}}) \right\|_2\right) \\ & \stackrel{b}{\leq} m_Q^{1/2} \sum_{j=n_t+1}^{t'} \eta_j O(\|\mathbf{P}(S_j \in \cdot) - \mathbf{P}_{\pi_{\theta_t}}\|_{TV} + \|\boldsymbol{\theta}_j - \boldsymbol{\theta}_t\|_2), \end{aligned} \quad (59)$$

where (59)-a uses the bounded property of  $\boldsymbol{\Delta}^{\omega_{j-1}}$  and  $\mathbf{M}^{m_{j-1}}$  and follows from triangle inequality. Moreover, (59)-b comes from that the policy  $\pi_{\theta}$  follows the Lipschitz conti-

nuity over  $\boldsymbol{\theta}$ . For the first term of (59)-b, we have

$$\begin{aligned} & \|\mathbf{P}(S_j \in \cdot) - \mathbf{P}_{\pi_{\theta_t}}\|_{TV} \\ & = \|\mathbf{P}(S_j \in \cdot) - \mathbf{P}_{\pi_{\theta_{j-\tau_j}}}\|_{TV} + \|\mathbf{P}_{\pi_{\theta_{j-\tau_j}}} - \mathbf{P}_{\pi_{\theta_t}}\|_{TV} \\ & \stackrel{a}{\leq} \lambda \rho^{\tau_j} + (\lceil \log_{\rho} \lambda^{-1} \rceil + \frac{1}{1-\rho}) O\left(\sum_{k=j-\tau_j+1}^t \beta_k\right), \end{aligned} \quad (60)$$

where (60)-a follows the ergodicity assumption and the theoretical result of (35) and (36) in [7], and we let  $\rho^{\tau_j} = O(\frac{1}{t})$ . Moreover, for the second term of (59)-b, we have

$$\|\boldsymbol{\theta}_j - \boldsymbol{\theta}_t\|_2 = O\left(\sum_{k=j+1}^t \beta_k\right). \quad (61)$$

By plugging (60) and (61) into (59), we obtain

$$\begin{aligned} & \|\mathbb{E}[\mathbf{m}_{t'}] - \mathbb{E}[\boldsymbol{\omega}_{t'}]\|_2 \\ & \leq m_Q^{1/2} \sum_{j=n_t+1}^{t'} O\left(\eta_j \lambda \rho^{\tau_j} + \eta_j \sum_{k=j-\tau_j+1}^t \beta_k\right) \\ & \leq O\left(m_Q^{1/2} \eta_{n_t} t^{\kappa_5-1} + m_Q^{1/2} \eta_{n_t} \beta_{n_t} t^{2\kappa_5}\right), \end{aligned} \quad (62)$$

Thus, we have  $e_{n_t}^b \leq m_Q^{1/2} \eta_{n_t} O(t^{-1} \delta_t^{-1} + \beta_{n_t} \delta_t^{-2})$ , and further have

$$\|\mathbb{E}[\bar{\mathbf{m}}_t] - \mathbb{E}[\bar{\boldsymbol{\omega}}_t]\|_2 \leq m_Q^{1/2} \eta_{n_t} O(t^{\kappa_5-1} + \beta_{n_t} t^{2\kappa_5}). \quad (63)$$

Combining (41), (42), (43), (47), (57), and (63), we can finally obtain

$$\begin{aligned} & \left| \mathbb{E}[f(\bar{\boldsymbol{\omega}}_t^i)] - \hat{Q}_i^{\pi_{\theta_t}} \right| \leq O\left(\frac{(1 - \gamma_t)^{t^{\kappa_5}/2}}{\gamma_t^{1/2}} + m_Q \eta_{n_t} t^{\kappa_5-1} \right. \\ & \quad \left. + m_Q \gamma_{n_t}^{1/2} \eta_{n_t}^{1/2} t^{\kappa_5/2} + \frac{\gamma_{n_t}^{1/2}}{\eta_{n_t}^{1/2}} + m_Q \eta_{n_t} \beta_{n_t} t^{2\kappa_5} + \epsilon_{m_Q}\right), \end{aligned} \quad (64)$$

with probability at least  $1 - L^2 \exp\{-a_9 m_Q R_{\omega}^{2/3} L\}$ . Finally, by setting  $\kappa_5 = 0.43$  in particular, we can finally obtain the theoretical result in Lemma 1. This completes the proof.

## APPENDIX C PROOF OF LEMMA 2

Our proof of Lemma 2 relies on a technical lemma [52, Lemma 1], which is restated below for completeness.

*Lemma 4.* Let  $(\Omega, \mathcal{G}, \mathbb{P})$  denote a probability space and let  $\{\mathcal{G}_t\}$  denote an increasing sequence of  $\sigma$ -field contained in  $\mathcal{G}$ . Let  $\{z^t\}, \{w^t\}$  be sequences of  $\mathcal{G}_t$ -measurable random vectors satisfying the relations

$$\begin{aligned} & w^{t+1} = \prod_{\mathcal{W}} (w^t + \alpha_t (\varrho^t - w^t)) \\ & \mathbb{E}[\varrho^t | \mathcal{G}_t] = z^t + o^t \end{aligned} \quad (65)$$

where  $\alpha_t \geq 0$  and the set  $\mathcal{W}$  is convex and closed,  $\prod_{\mathcal{W}}(\cdot)$  denotes projection on  $\mathcal{W}$ . Let

- (a) all accumulation points of  $\{w^t\}$  belong to  $\mathcal{W}$  w.p.l.,
  - (b) there is a constant  $C$  such that  $\mathbb{E}[\|\varrho^t\|_2 | \mathcal{G}_t] \leq C, \forall t \geq 0$ ,
  - (c)  $\sum_{t=0}^{\infty} \mathbb{E}[(\alpha_t)^2 + \alpha_t \|o^t\|] < \infty$
  - (d)  $\sum_{t=0}^{\infty} \alpha_t = \infty$ , and (e)  $\|w^{t+1} - w^t\|/\alpha_t \rightarrow 0$  w.p.l.,
- Then  $z^t - w^t \rightarrow 0$  w.p.l.

By Lemma 5, we can prove the asymptotic consistency of function values (28) following the similar analyses in

Appendix A-A of [7], and we omit the proof due to the space limit. Then we give the proof of (29).

We first construct an auxiliary policy gradient estimate:

$$\nabla_{\theta} \hat{J}_i(\theta) = \mathbb{E}_{\sigma_{\pi_{\theta}}} \left[ \hat{Q}_i^{\pi_{\theta}}(s, \mathbf{a}) \nabla_{\theta} \log \pi_{\theta}(\mathbf{a} | s) \right], \forall i, \quad (66)$$

Note that the only difference between (18) and (66) is that we replace the exact Q-value  $Q_i^{\pi_{\theta_t}}$  with the approximate Q-functions  $\hat{Q}_i^{\pi_{\theta_t}}$ . Then the asymptotic consistency of (29) can be decomposed into the following two steps:

$$\text{Step1: } \lim_{t \rightarrow \infty} \left\| \nabla_{\theta} \hat{J}_i(\theta) - \nabla_{\theta} J_i(\theta_t) \right\|_2 = 0 \quad (67)$$

$$\text{Step2: } \lim_{t \rightarrow \infty} \left\| \hat{g}_i^t - \nabla_{\theta} \hat{J}_i(\theta) \right\|_2 \leq \epsilon_{m_Q} \quad (68)$$

a) *Step 1*: Combining (18) with (66), and together with the regularity conditions in Assumption 1, i.e.,  $C'_i$  and  $\nabla_{\theta} \log \pi_{\theta}$  are bounded, we have

$$\left\| \nabla_{\theta} \hat{J}_i(\theta_t) - \nabla_{\theta} J_i(\theta_t) \right\|_2 = O(\left\| \hat{J}_i^t - J_i(\theta_t) \right\|_2). \quad (69)$$

Recalling (28), we can complete the proof of step 1.

b) *Step 2*: Since the step size  $\{\alpha_t\}$  follows Assumption 3, and  $C_i(s, \mathbf{a}), \forall i$  is bounded, it's easy to prove that the conditions (a), (b), and (d) in Lemma 4 are satisfied. Now, we are ready to prove the technical condition (c).

Together with the definition of real gradient  $\nabla J_i(\theta_t)$  in (18), we obtain the stochastic policy gradient error:

$$\begin{aligned} \left\| o^t \right\|_2 &= \left\| \hat{g}_i^{t+1} - \nabla_{\theta} J_i(\theta_t) \right\|_2 \quad (70) \\ &\stackrel{a}{=} \frac{1}{T_t} \sum_{l=1}^{T_t} O(\left\| \theta_t - \theta_{t-T_t+l} \right\|_2 + \left\| \mathbf{P}(S_{t-T_t+l} \in \cdot) - \mathbf{P}_{\pi_{\theta_t}} \right\|_{TV} \\ &\quad + \left| \mathbb{E}[\hat{f}(\bar{\omega}_t^i)] - \hat{Q}_i^{\pi_{\theta_t}} \right|), \end{aligned}$$

where (70)-a follows from similar tricks as in (59), triangle inequality, and the regularity conditions in Assumption 1, i.e., the policy  $\pi_{\theta}$  follows the Lipschitz continuity over  $\theta$ , and  $C'_i$ , the output of DNNs and  $\nabla_{\theta} \log \pi_{\theta}$  are bounded. Then, plugging (60), (61) and Lemma 1 into (70), we finally obtain

$$\begin{aligned} \left\| o^t \right\|_2 &= O(\epsilon_{m_Q} + t^{-1} + T_t \beta_{t-T_t} + \frac{(1-\gamma_t)^{t^{\kappa_5}/2}}{\gamma_t^{1/2}} + \frac{\gamma_{n_t}^{1/2}}{\eta_{n_t}^{1/2}} \\ &\quad + m_Q \gamma_{n_t}^{1/2} \eta_{n_t}^{1/2} t^{\kappa_5/2} + m_Q \eta_{n_t} t^{\kappa_5-1} + m_Q \eta_{n_t} \beta_{n_t} t^{2\kappa_5}), \quad (71) \end{aligned}$$

where we set  $\rho^{\tau_t} = O(\frac{1}{t})$ , which means  $\tau_t = O(\log t)$ . According to Assumption 2, it's easy to prove that condition (c) is held. For the condition (e), we have

$$\begin{aligned} \left\| \nabla_{\theta} \hat{J}_i(\theta_{t+1}) - \nabla_{\theta} \hat{J}_i(\theta_t) \right\|_2 &\quad (72) \\ &= O(\left\| \theta_{t+1} - \theta_t \right\|_2 + \left\| \mathbf{P}_{\pi_{\theta_{t+1}}} - \mathbf{P}_{\pi_{\theta_t}} \right\|_{TV}) = O(\beta_t) \end{aligned}$$

It can be seen from Assumption 2 that technical condition (e) is also satisfied. This completes the proof of step 2.

## REFERENCES

- [1] K. Arulkumaran, M. P. Deisenroth, M. Brundage, and A. A. Bharath, "Deep reinforcement learning: A brief survey," *IEEE Trans. Signal Process.*, vol. 34, no. 6, pp. 26–38, 2017.
- [2] D. Silver, A. Huang, C. J. Maddison, A. Guez, L. Sifre, G. Van Den Driessche, J. Schrittwieser, I. Antonoglou, V. Panneershelvam, M. Lanctot *et al.*, "Mastering the game of Go with deep neural networks and tree search," *Nature*, vol. 529, no. 7587, pp. 484–489, 2016.
- [3] V. Mnih, K. Kavukcuoglu, D. Silver, A. Graves, I. Antonoglou, D. Wierstra, and M. Riedmiller, "Playing Atari with deep reinforcement learning," 2013.
- [4] T. W. Bickmore, H. Trinh, S. Olafsson, T. K. O'Leary, R. Asadi, N. M. Rickles, and R. Cruz, "Patient and consumer safety risks when using conversational assistants for medical information: an observational study of Siri, Alexa, and Google assistant," *J Med Internet Res*, vol. 20, no. 9, p. e11510, 2018.
- [5] J. Schulman, S. Levine, P. Abbeel, M. Jordan, and P. Moritz, "Trust region policy optimization," in *ICML*. PMLR, 2015, pp. 1889–1897.
- [6] C.-X. Wang, J. Wang, S. Hu, Z. H. Jiang, J. Tao, and F. Yan, "Key technologies in 6G terahertz wireless communication systems: A survey," *IEEE Veh. Technol. Mag.*, vol. 16, no. 4, pp. 27–37, 2021.
- [7] C. Tian, A. Liu, G. Huang, and W. Luo, "Successive convex approximation based off-policy optimization for constrained reinforcement learning," *IEEE Trans. Signal Process.*, vol. 70, pp. 1609–1624, 2022.
- [8] J. Zhang, A. S. Bedi, M. Wang, and A. Koppel, "Cautious reinforcement learning via distributional risk in the dual domain," *IEEE Journal on Selected Areas in Information Theory*, vol. 2, no. 2, pp. 611–626, 2021.
- [9] J. Zhang, A. Koppel, A. S. Bedi, C. Szepesvari, and M. Wang, "Variational policy gradient method for reinforcement learning with general utilities," in *Advances in Neural Information Processing Systems*, H. Larochelle, M. Ranzato, R. Hadsell, M. Balcan, and H. Lin, Eds., vol. 33. Curran Associates, Inc., 2020, pp. 4572–4583.
- [10] D. Ding, K. Zhang, T. Basar, and M. R. Jovanovic, "Convergence and optimality of policy gradient primal-dual method for constrained markov decision processes," in *2022 American Control Conference (ACC)*, 2022, pp. 2851–2856.
- [11] Y. Chen, J. Dong, and Z. Wang, "A primal-dual approach to constrained markov decision processes," *arXiv preprint arXiv:2101.10895*, 2021.
- [12] D. Ding, K. Zhang, T. Basar, and M. Jovanovic, "Natural policy gradient primal-dual method for constrained markov decision processes," *Advances in Neural Information Processing Systems*, vol. 33, pp. 8378–8390, 2020.
- [13] A. Stooke, J. Achiam, and P. Abbeel, "Responsive safety in reinforcement learning by pid lagrangian methods," in *International Conference on Machine Learning*. PMLR, 2020, pp. 9133–9143.
- [14] D. Ding, X. Wei, Z. Yang, Z. Wang, and M. Jovanovic, "Provably efficient safe exploration via primal-dual policy optimization," in *International Conference on Artificial Intelligence and Statistics*. PMLR, 2021, pp. 3304–3312.
- [15] A. Muller, P. Alatur, G. Ramponi, and N. He, "Cancellation-free regret bounds for lagrangian approaches in constrained markov decision processes," 2023.
- [16] D. Ding, C.-Y. Wei, K. Zhang, and A. Ribeiro, "Last-iterate convergent policy gradient primal-dual methods for constrained mdps," 2023.
- [17] J. Achiam and D. Amodei, "Benchmarking safe exploration in deep reinforcement learning," 2019.
- [18] M. Gaur, A. S. Bedi, D. Wang, and V. Aggarwal, "On the global convergence of natural actor-critic with two-layer neural network parametrization," *arXiv preprint arXiv:2306.10486*, 2023.
- [19] Z. Yang, Y. Chen, M. Hong, and Z. Wang, "Provably global convergence of actor-critic: A case for linear quadratic regulator with ergodic cost," *Advances in neural information processing systems*, vol. 32, 2019.
- [20] B. Liu, Q. Cai, Z. Yang, and Z. Wang, "Neural proximal/trust region policy optimization attains globally optimal policy," *arXiv preprint arXiv:1906.10306*, 2019.
- [21] Q. Liang, F. Que, and E. Modiano, "Accelerated primal-dual policy optimization for safe reinforcement learning," *arXiv preprint arXiv:1802.06480*, 2018.
- [22] S. Paternain, L. Chamon, M. Calvo-Fullana, and A. Ribeiro, "Constrained reinforcement learning has zero duality gap," in *Advances in Neural Information Processing Systems*, H. Wallach, H. Larochelle, A. Beygelzimer, F. d'Alché-Buc, E. Fox, and R. Garnett, Eds., vol. 32. Curran Associates, Inc., 2019.
- [23] J. Achiam, D. Held, A. Tamar, and P. Abbeel, "Constrained policy optimization," in *ICML*. PMLR, 2017, pp. 22–31.
- [24] S. Zou, T. Xu, and Y. Liang, "Finite-sample analysis for sarsa with linear function approximation," *Adv. Neural Inf. Process. Syst.*, vol. 32, 2019.
- [25] Z. Liu, Z. Guo, Y. Yao, Z. Cen, W. Yu, T. Zhang, and D. Zhao, "Constrained decision transformer for offline safe reinforcement learning," in *International Conference on Machine Learning*. PMLR, 2023, pp. 21 611–21 630.
- [26] Y. F. Wu, W. ZHANG, P. Xu, and Q. Gu, "A finite-time analysis of two time-scale actor-critic methods," in *Advances in Neural Information Processing Systems*, H. Larochelle, M. Ranzato, R. Hadsell, M. Balcan, and H. Lin, Eds., vol. 33. Curran Associates, Inc., 2020, pp. 17 617–17 628.
- [27] X. Chen, J. Duan, Y. Liang, and L. Zhao, "Global convergence of two-timescale actor-critic for solving linear quadratic regulator," in *Proceedings of the AAAI Conference on Artificial Intelligence*, vol. 37, no. 6, 2023, pp. 7087–7095.

- [28] T. Xu, Z. Wang, and Y. Liang, “Non-asymptotic convergence analysis of two time-scale (natural) actor-critic algorithms,” *arXiv preprint arXiv:2005.03557*, 2020.
- [29] X. Chen and L. Zhao, “Finite-time analysis of single-timescale actor-critic,” 2023.
- [30] A. Destounis and G. S. Paschos, “Complexity of URLLC scheduling and efficient approximation schemes,” in *Proc. Int. Symp. Modeling and Optim. Mobile, Ad Hoc, and Wireless Netw. (WiOPT)*, 2019, pp. 1–8.
- [31] X. Zhao, Y.-J. A. Zhang, M. Wang, X. Chen, and Y. Li, “Online multi-user scheduling for xr transmissions with hard-latency constraint: Performance analysis and practical design,” *IEEE Trans. Commun.*, 2024.
- [32] H. Ren, C. Pan, Y. Deng, M. ElKashlan, and A. Nallanathan, “Resource allocation for secure URLLC in mission-critical IoT scenarios,” *IEEE Trans. Commun.*, vol. 68, no. 9, pp. 5793–5807, 2020.
- [33] C. B. Peel, B. M. Hochwald, and A. L. Swindlehurst, “A vector-perturbation technique for near-capacity multiantenna multiuser communication-part I: channel inversion and regularization,” *IEEE Trans. Commun.*, vol. 53, no. 1, pp. 195–202, 2005.
- [34] B. Recht, “A tour of reinforcement learning: The view from continuous control,” *Annu. Rev. Control, Robot., Auton. Syst.*, vol. 2, pp. 253–279, 2019.
- [35] M. Fazel, R. Ge, S. Kakade, and M. Mesbahi, “Global convergence of policy gradient methods for the linear quadratic regulator,” in *ICML*. PMLR, 2018, pp. 1467–1476.
- [36] C.-Y. Wei, M. J. Jahromi, H. Luo, H. Sharma, and R. Jain, “Model-free reinforcement learning in infinite-horizon average-reward markov decision processes,” in *International conference on machine learning*. PMLR, 2020, pp. 10 170–10 180.
- [37] Y. Cao and Q. Gu, “Generalization error bounds of gradient descent for learning over-parameterized deep relu networks,” in *Proc. AAAI Conf. Artif. Intell.*, vol. 34, no. 04, 2020, pp. 3349–3356.
- [38] Z. Allen-Zhu, Y. Li, and Z. Song, “A convergence theory for deep learning via over-parameterization,” in *ICML*. PMLR, 2019, pp. 242–252.
- [39] Y. Cao and Q. Gu, “Generalization bounds of stochastic gradient descent for wide and deep neural networks,” *Proc. Adv. Neural Inf. Process. Syst.*, vol. 32, 2019.
- [40] R. S. Sutton and A. G. Barto, *Reinforcement learning: An introduction*. MIT press, 2018.
- [41] P. Xu and Q. Gu, “A finite-time analysis of Q-learning with neural network function approximation,” in *ICML*. PMLR, 2020, pp. 10 555–10 565.
- [42] S. Qiu, Z. Yang, J. Ye, and Z. Wang, “On finite-time convergence of actor-critic algorithm,” *IEEE J. Sel. Areas Inf. Theory*, vol. 2, no. 2, pp. 652–664, 2021.
- [43] A. Koloskova, H. Hendrikx, and S. U. Stich, “Revisiting gradient clipping: Stochastic bias and tight convergence guarantees,” in *Proceedings of the 40th International Conference on Machine Learning*, ser. Proceedings of Machine Learning Research, vol. 202. PMLR, 23–29 Jul 2023, pp. 17 343–17 363.
- [44] J. Qian, Y. Wu, B. Zhuang, S. Wang, and J. Xiao, “Understanding gradient clipping in incremental gradient methods,” in *International Conference on Artificial Intelligence and Statistics*. PMLR, 2021, pp. 1504–1512.
- [45] X. Glorot and Y. Bengio, “Understanding the difficulty of training deep feedforward neural networks,” in *Proceedings of the thirteenth international conference on artificial intelligence and statistics*. JMLR Workshop and Conference Proceedings, 2010, pp. 249–256.
- [46] R. S. Sutton and A. G. Barto, *Reinforcement learning: An introduction*. MIT press, 2018.
- [47] A. Liu, V. K. N. Lau, and B. Kananian, “Stochastic successive convex approximation for non-convex constrained stochastic optimization,” *IEEE Trans. Signal Process.*, vol. 67, no. 16, pp. 4189–4203, 2019.
- [48] J. Fan, Z. Wang, Y. Xie, and Z. Yang, “A theoretical analysis of deep Q-learning,” in *Proc. Learn. Dyn. Control*. PMLR, 2020, pp. 486–489.
- [49] S. Tosatto, M. Pirota, C. d’Eramo, and M. Restelli, “Boosted fitted Q-iteration,” in *ICML*. PMLR, 2017, pp. 3434–3443.
- [50] A. Liu, R. Yang, T. Q. S. Quek, and M.-J. Zhao, “Two-stage stochastic optimization via primal-dual decomposition and deep unrolling,” *IEEE Trans. Signal Process.*, vol. 69, pp. 3000–3015, 2021.
- [51] M. Yu, Z. Yang, M. Kolar, and Z. Wang, “Convergent policy optimization for safe reinforcement learning,” *Adv. Neural Inf. Process. Syst.*, vol. 32, 2019.
- [52] A. Ruszczyński, “Feasible direction methods for stochastic programming problems,” *Math. Program.*, vol. 19, pp. 220–229, 1980.